



Since January 2020 Elsevier has created a COVID-19 resource centre with free information in English and Mandarin on the novel coronavirus COVID-19. The COVID-19 resource centre is hosted on Elsevier Connect, the company's public news and information website.

Elsevier hereby grants permission to make all its COVID-19-related research that is available on the COVID-19 resource centre - including this research content - immediately available in PubMed Central and other publicly funded repositories, such as the WHO COVID database with rights for unrestricted research re-use and analyses in any form or by any means with acknowledgement of the original source. These permissions are granted for free by Elsevier for as long as the COVID-19 resource centre remains active.



Understanding the heterogeneity of COVID-19 deaths and contagions: The role of air pollution and lockdown decisions[☆]

Leonardo Becchetti^a, Gianluigi Conzo^a, Pierluigi Conzo^{b,*}, Francesco Salustri^c

^a University of Rome "Tor Vergata", Italy

^b University of Turin & Collegio Carlo Alberto, Italy

^c University College London, United Kingdom

ARTICLE INFO

JEL classification:

I18

Q53

J18

H12

Keywords:

COVID-19 pandemic

Particulate matter

Lockdown

Economic activity

ABSTRACT

The uneven geographical distribution of the novel coronavirus epidemic (COVID-19) in Italy is a puzzle given the intense flow of movements among the different geographical areas before lockdown decisions. To shed light on it, we test the effect of the quality of air (as measured by particulate matter and nitrogen dioxide) and lockdown restrictions on daily adverse COVID-19 outcomes during the first pandemic wave in the country. We find that air pollution is positively correlated with adverse outcomes of the pandemic, with lockdown being strongly significant and more effective in reducing decreases in more polluted areas. Results are robust to different methods including cross-section, pooled and fixed-effect panel regressions (controlling for spatial correlation), instrumental variable regressions, and difference-in-differences estimates of lockdown decisions through predicted counterfactual trends. They are consistent with the consolidated body of literature in previous medical studies suggesting that poor quality of air creates chronic exposure to adverse outcomes from respiratory diseases. The estimated correlation does not change when accounting for other factors such as temperature, commuting flows, quality of regional health systems, share of public transport users, population density, the presence of Chinese community, and proxies for industry breakdown such as the share of small (artisan) firms. Our findings provide suggestions for investigating uneven geographical distribution patterns in other countries, and have implications for environmental and lockdown policies.

1. Introduction

Viruses do not travel alone. They take human beings as means of transport. For this reason, the heterogeneity of the diffusion of the novel coronavirus (SARS-CoV-2, thereafter coronavirus) in Italy is puzzling. As is well known contagions and deaths in Italy during the first pandemic wave were disproportionately concentrated in some provinces of a single region (Lombardia) and, more in general, in the North of Italy (Piemonte and Emilia-Romagna).¹ Several authors emphasize that the

coronavirus was circulating at least since early January and well before late February 2020, when the first cases were detected (e.g. Zehender et al., 2020).² The month before the country lockdown, when the government limited people movement around the country,³ the flow of commuting between Rome and Milan was intense, as it has always been in these last years with flight and high-speed train connections allowing to move from one city to another in slightly less than 3 hours. If the virus easily jumped from the remote Wuhan to Milan, it is reasonable to wonder why it did not do so across a much shorter distance, i.e. that

[☆] We thank Kaushik Basu, Valeria Di Cosmo, Phoebe Kounduri, Marilena Locatelli, Koen Pouwels, Jeffrey Sachs, Alberto Vassallo and all the participants to the webinar of the Italian Economics Association held in 2020 for their comments and suggestions. The usual disclaimer applies.

* Corresponding author. Dept. of Economics & Statistics "Cognetti de Martini", University of Turin, Lungodora Siena 100A, 10153, Torino, Italy.

E-mail address: Pierluigi.conzo@unito.it (P. Conzo).

¹ As of June 17th 2020, Lombardia accounted for 38.8 percent of reported contagions and 49 percent of registered COVID-19 deaths.

² The authors show that epidemiological tracing, based on phylogenetic analysis of the first three complete genomes of SARS-CoV-2 isolated from three patients involved in the first outbreak of COVID-19 in Lombardy, provided evidence that SARS-CoV-2 was present in Italy weeks before the first reported cases of infection.

³ The decree on the full restriction of movement among regions was enacted only on 11th March 2020. The information spillover before the decree was operating led to mass escape from Milan train station toward Southern Italy the days before (see <https://www.milanopost.info/2020/03/09/234982/>).

between Milan and Rome or, more in general, between the North and the South of Italy.⁴⁵

An interesting research question is therefore why the intensity of the epidemic (hereon COVID-19) has been so different between different Italian provinces. A first tentative answer is that the virus was not spreading in Rome or in the Center-South before the government restrictions. Those restrictions were therefore crucial to limit the epidemic in these areas, although the anecdotal evidence reported above casts some doubts about this first hypothesis. The second tentative answer is that the virus travelled way before the first lockdown, and some concurring factors like pollution, weather conditions, or less intense economic activity made it weaker in areas located distant from the “epicenter”.

Our paper aims to shed light on this puzzle by investigating the relative role of quality of air in explaining the spread of epidemic in Italy during the first pandemic wave, and its interaction with lockdown decisions. The focus of our research has relevant implications on several dimensions such as subjective wellbeing, health policies, economic conditions and economic policies, not ultimately since – as of June 17th, 2020 – the epidemic in Italy caused 34,448 official deaths, stressed the national health system and produced a paralysis of economic activity.⁶

Our empirical approach rests on a multivariate analysis which aims to add original insights from at least three points of view. First, assessing the relative strength of different concurring factors – i.e. demographic structure, human mobility, health system efficiency, quality of air, climate conditions, economic activity and lockdown measures – is fundamental to understand the heterogeneous evolution of the epidemic across the country. This approach is a necessary complement to deterministic models, in which nonlinear dynamics of the diffusion were used as a unique control. Second, lockdown decisions have highlighted the trade-off between health and economic development goals.

Our findings suggest that the first lockdown measures mitigated contagions and mortality, especially in the more polluted areas. Conversely, poor quality of air and the share of small business activity are positively correlated with both outcomes. Finally, the heterogeneity of diffusion does not seem to depend on other pre-pandemic factors that we test, i.e. commuting and public transport use, health system efficiency, density and the share of Chinese immigrants.

The paper is divided into eight sections. In the second section we present our research hypotheses and the related literature. In the third section we illustrate data and econometric model. In the fourth we present descriptive and econometric findings. In the fifth section, using pre-lockdown data we build a counterfactual trend and use a difference-in-differences approach to evaluate the impact of lockdown, and its interaction with pollution, at municipality level. In the sixth section we implement a series of robustness checks including instrumental variable regressions. In the seventh section we discuss our results (limits, policy implications and directions for future research). The eighth section concludes.

⁴ On 31st January 2020 a couple of Chinese tourists who had spent some days in Milan, Parma and Rome (since 28th of January) was recovered in serious conditions at the Spallanzani hospital in Rome (<https://www.ilgiornale.it/news/roma/allarme-albergo-mio-marito-ha-febbre-1819431.html>).

⁵ The flow of passengers moving from Rome to Milan (airplane plus train) was around 5.14 million in 2018. 3.6 million by train, which is the 70% of the total passengers, the others are by plane (20%) and by car (10%). Sources: https://www.fsitaliane.it/content/dam/fsitaliane/Documents/fsnews/comunicati-stampa/2019/dicembre/2019_12_05_NS_2_FS_Italiane_10_anni_AV_cambiato_Paese_e_vita_personale.pdf; <https://www.ilsole24ore.com/art/roma-milano-7-passeggeri-10-scelgono-treno-AEOuGL5>.

⁶ According to the National Institute of Statistics preliminary estimates, the Italian GDP fell by 4.7% in the first quarter causing around 8 million temporary layoffs (<https://www.istat.it/it/archivio/242084>).

2. Background and research hypotheses

The first hypothesis we test is that *the lockdown measures proved effective in limiting deceases and contagion* (H_1) during the first pandemic wave. Human mobility restrictions are considered among the most effective policies to reduce contagion in absence of a vaccine, but their economic costs are huge (Bajardi et al., 2011; Wang and Taylor, 2016; Charu et al., 2017). Fang et al. (2020) calculate that contagion cases would be 64.81% higher in the 347 Chinese cities outside Hubei province, and 52.64% higher in the 16 non-Wuhan cities inside Hubei, without the Wuhan lockdown. The coronavirus mean incubation period, defined as the time from infection to illness onset, has been estimated at 5.2 days (4.1–7.0), with the 95th percentile of the distribution at 12.5 days (Li et al., 2020). Moreover, the majority of people were tested with severe symptoms only (as International guidelines suggested) and with some delay with respect to the day in which the test was recorded (3.6 days according to Cereda et al., 2020). We therefore expect that governmental restrictions reducing the flow of human interactions and imposing physical distance among people have an impact, which may be distributed over around 17 days. Thus, we test the effect of the different national, regional, and provincial measures enacted in Italy in the months of coronavirus outbreak. Table 1 lists the restrictions adopted at different governmental levels.

The second hypothesis we test is that *(historical levels of) particulate matter has a positive and significant role in explaining the geographic variation of the epidemic* (H_2). There are two hypotheses on pollution as a pull factor of COVID-19. The first is that individuals living in highly polluted areas have weaker lungs and reduced capacity to react to respiratory diseases and/or pneumonias and, therefore, also to COVID-19. The second is that particular matter is a carrier of the virus, slowing down its falls from the air (Piazzalunga-Expert, 2020). The rationale for the first hypothesis is that lung reaction to pneumonia depends on the pulmonary surfactant (a surface-active lipoprotein complex formed by type II alveolar cells). The pulmonary surfactant contributes with minimal diffusion distance and large surface area to the optimal exchange of gases. In essence, a healthy surfactant protects lung collapse at low volumes and tissue damage at high volume levels and allows lungs to inflate much more easily, thereby reducing the work of breathing. Pollution and heavy smoke produce abnormalities in surfactant composition, thereby making ventilation more problematic and reducing lung “efficiency” (Pastva et al., 2007).

The hypothesis has been tested and not rejected by a large body of literature finding correlations between pollution and pneumonia not only for the children but also for the elders. Neupane et al. (2010) find that PM_{2.5} is significantly associated with hospitalization for pneumonia in Canada, Medina-Ramon et al. (2006) find that PM₁₀ is associated with hospitalization for respiratory diseases in 36 US cities. Xu et al. (2016) obtain similar results in a Chinese sample, while Zanobetti and Schwartz (2006) in Boston. Luginaah et al. (2005) report significant correlation between (PM₁₀ and PM_{2.5}), NO₂, SO₂, and disease exacerbations, emergency admissions, hospitalizations and mortality in Ontario.

Some of this research has been conducted before the coronavirus outbreak in the areas where the epidemic has been more severe. Zhang et al. (2015) find that local PM_{2.5} has an acute adverse effect on lung function in young healthy adults in Wuhan, with temperature also playing an important role. Santus et al. (2012) find an acute effect of CO, SO₂ and PM₁₀ on Emergency Rate Admissions for pneumonia in Milan at short daily lags. Zeng et al. (2016) find that smaller particles have been shown to have stronger effects on multiple respiratory diseases and increased hospitalization rates than larger ones; their sedimentation speed is, indeed, lower and exposition to them higher for the human body. Larger particles are filtered by nostrils while smaller ones can reach alveolar cells (Zeng et al., 2016). Pope and Dockery (2006) resume findings from this literature in their survey on more than 500 past studies arguing that the body of evidence on the nexus between

Table 1
Restriction policies.

Date	Restriction	Location	Source
February 23rd	Full lockdown at district level	Lombardia (Bertonico, Casalpusterlengo; Castelgerundo; Castiglione D'Adda; Codogno; Fombio, Maleo; San Fiorano, Somaglia, Terranova dei Passerini), Veneto (Vo').	https://www.gazzettaufficiale.it/eli/id/2020/02/23/20A01228/sg
February 25th	All public and private events and sport activities suspended; all school trips, monthly free access to museum suspended (national level)	Emilia Romagna, Friuli Venezia Giulia, Lombardia, Veneto, Liguria, Piemonte	https://www.gazzettaufficiale.it/eli/id/2020/02/25/20A01278/sg
March 1st	Partial lockdown (public events and schools suspended; other activities must ensure no big groups) Medium and Big-size enterprise closed on weekends	Emilia Romagna, Lombardia, Veneto; Pesaro e Urbino, Savona, Bergamo, Lodi, Piacenza, Cremona	https://www.gazzettaufficiale.it/eli/id/2020/03/01/20A01381/sg
March 4th	Public and private events suspended, smart working highly encouraged, elderly and unhealthy recommended to stay home, Lockdown of schools and universities and partial limitations	Italy	https://www.gazzettaufficiale.it/eli/id/2020/03/04/20A01475/sg
March 8th	Full lockdown	Lombardia, Modena, Parma, Piacenza, Reggio nell'Emilia, Rimini, Pesaro e Urbino, Alessandria, Asti, Novara, Verbano-Cusio-Ossola, Vercelli, Padova, Treviso, Venezia.	https://www.gazzettaufficiale.it/eli/id/2020/03/08/20A01522/sg
March 10th	Full lockdown	Italy	http://www.governo.it/it/articolo/firmato-il-dpcm-9-marzo-2020/14276#

particulate matter and respiratory and pulmonary diseases is stronger if we look at long run exposure.

A few very recent papers focus directly on the relationship between pollution and COVID-19 disease. [Wu et al. \(2020\)](#) find that long-term average exposure to fine particulate matter (PM_{2.5}) increases the risk of COVID-19 deaths in the United States (in terms of economic magnitude they find that an increase of 1 µg/m³ in PM_{2.5} is associated with a 15% increase in the COVID-19 death rate). [Conticini, Frediani and Caro \(2020\)](#) argue that pollution can be a co-determinant of the abnormal number of deaths registered in Lombardia and Emilia Romagna. The authors emphasize how the composed air quality index including five pollutants (PM₁₀, PM_{2.5}, O₃, SO₂ and NO₂) show that Lombardia and Emilia Romagna are the most polluted in Italy and among the most polluted in Europe). The authors provide medical details on how poor air quality leads to inflammation, eventually leading to an innate immune system hyper-activation, which has been observed in COVID-19 patients. They also report how particulate matter (PM_{2.5} and PM₁₀) can lead to systemic inflammation consisting of an overexpression of PDGF, VEGF, TNFα, IL-1 and IL-6 which can arise even in healthy, non-smoker and young subjects ([Pope et al., 2009](#)). The effect is directly related to the length of pollutant exposure ([Tsai et al., 2019](#)). They conclude that the elderly who live in the regions with higher intensity of particulate suffered from chronic exposure to air pollution and have higher probability of being affected by virus invasion due to the weakened upper airways defenses.

[Fig. 1](#) shows the geographical distribution of COVID-19 related outcomes and of average levels of PM₁₀ and PM_{2.5} in Italy. Indeed, the cumulative number of positive cases and deaths per 1,000 inhabitants as of April 15th 2020 tend to concentrate in provinces that witnessed high levels of pollution in 2018, i.e. those in the North of Italy.

Finally, we also test the relative role of other pre-pandemic factors that might be associated with the COVID-19 outbreak and with its outcomes. We look at human mobility and density since these factors increase the chances of social interaction and hence the spread of the virus. In addition, we account for the heterogeneous efficiency of the local health system across Italian provinces. We also control for the demographic structure of the virus by including in the multivariate analysis also the share of residents aged over 65, because this age group has been shown to be more vulnerable to the virus. Finally, we also test the role of the Chinese community in Italy, since its presence could capture some of the socio-economic exchanges between Italy and China before the outbreak of the virus. It has also to be noted that the Chinese

presence in Italy has been connected to the spread of the virus in Italian provinces by anti-immigration supporters. Moreover, Chinese people residing in Italy have been frequently witnessed discrimination during the first days of the COVID-19 outbreak, under the form of physical and verbal violence.

3. Data and econometric model

Our database includes two dependent variables related to outcomes of the coronavirus disease and regressors including province time invariant characteristics, national or regional restriction events and time varying variables related to temperature and lockdown measures. As dependent variables we consider the daily number of deaths (released by the Italian National Statistics Institute, ISTAT) and new positive cases of COVID-19 at province level (from the Italian Civil Protection, ICP) per 1,000 inhabitants during the first pandemic wave in Italy.

The number of deaths is the daily number of deceases in 87% Italian municipalities covering 86% of Italian population.⁷ We use the daily number of deaths per 1,000 inhabitants of the municipality, from February 24th 2020 to April 15th, 2020 (the last date for which ISTAT data are available), averaged at province level.

The second dependent variable is the number of new daily confirmed COVID-19 cases, that is the number of new infected patients detected each day. We use this measure instead of the number of *net* infected patients, where deaths and recoveries of the day are subtracted from the gross value, because ICP does not provide the breakdown of infected patients at the province level (i.e. our main unit of analysis). Notwithstanding possible measurement errors that make the accounting more or less conservative (e.g. due to the region-specific testing capacity), one advantage of our research is that we limit the analysis to the Italian case, and therefore we avoid measurement bias arising from the different approaches followed in different countries. Since the accounting of positive cases is not voluntarily provided by provinces, but officially managed by a national institution and its local branches (ICP), we therefore expect that this potential source of measurement bias might not affect our estimates.

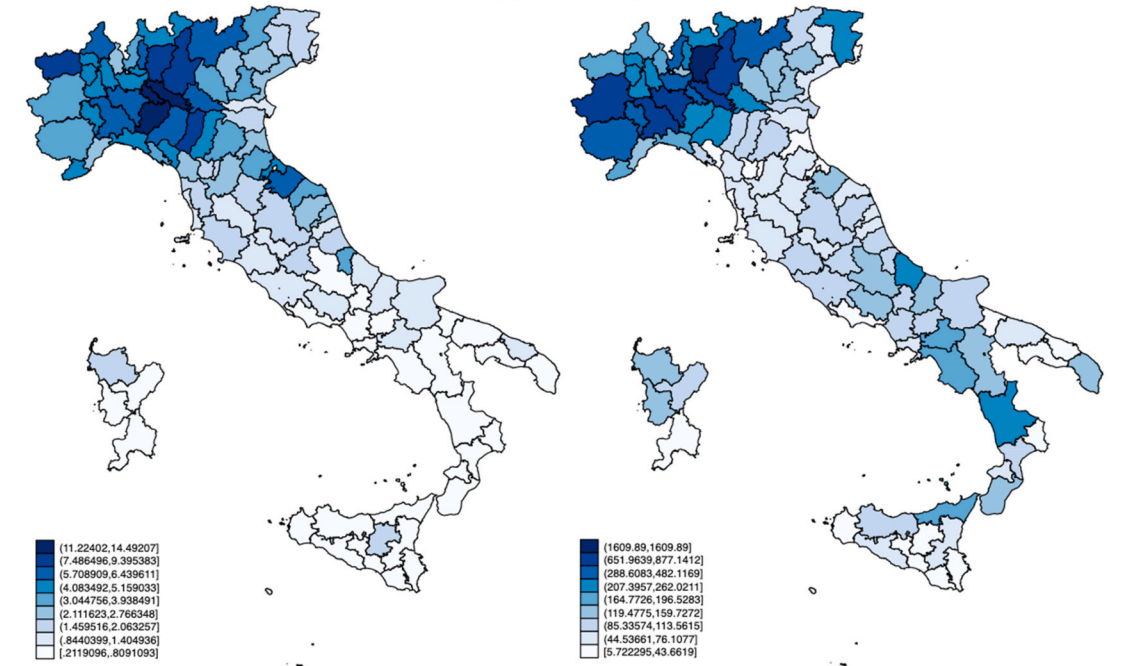
The fully-augmented model we consider is detailed in the following equation:

⁷ See https://www.istat.it/it/files//2020/05/Rapporto_Istat_ISS.pdf

Panel A: Total cases per 1000 inhabitants

[April 15th 2020]

Panel B: Total deaths per 1000 inhabitants



Panel C: average levels of PM10 in 2018

Panel D: average levels of PM2.5 in 2018

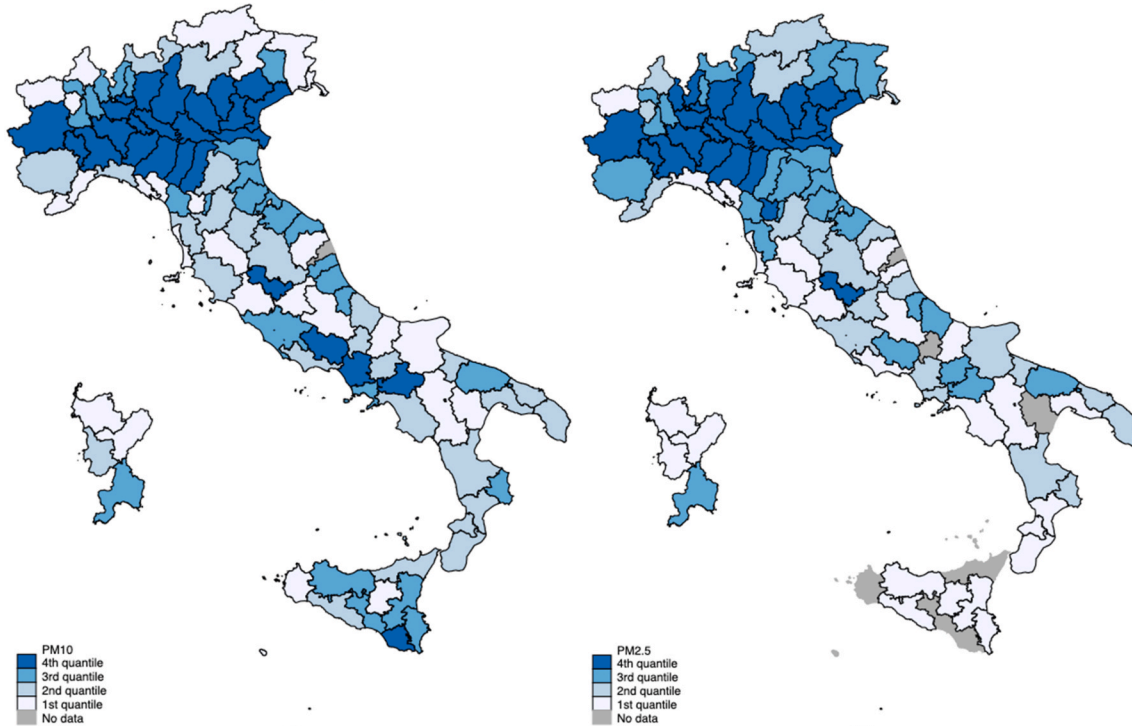


Fig. 1. COVID-19 contagion, mortality and pre-existing pollution levels.

$$\begin{aligned}
 CV19 - Outcome_{it} = & \alpha_0 + \alpha_1 Pollution_i + \alpha_2 UrbanGreen_i \\
 & + \alpha_3 HighTemperature_{it} + \alpha_4 Artisan_i + \alpha_5 Density_i \\
 & + \alpha_6 Income_i + \alpha_7 Over65_i + \alpha_8 Health_{pca\ i} \\
 & + \alpha_9 InternalCommunting_i + \alpha_{10} ExternalCommunting_i \\
 & + \alpha_{11} PublicTransportUse_i + u_{it}
 \end{aligned}$$

Eq.1

where $CV19 - Outcome$ is, in turn, the number of contagions over local population ($cases_{pc}$) or, alternatively, the number of deceases over local population ($deaths_{pc}$), both per 1,000 inhabitants in province i , and day t .

To test our research hypothesis on the impact of exposure to pollution before the outbreak of the virus, we use PM measures, that is, alternatively, PM2.5 and PM10, which are the two fine particulate

matter variables measuring average values in $\mu\text{g}/\text{m}^3$ registered by environmental monitoring units at province level in 2018. In alternative models, we also test the role of nitrogen dioxide (NO_2) in $\mu\text{g}/\text{m}^3$ as registered by environmental monitoring units at province level in 2018. Pollution variables are introduced as time-invariant local characteristics based on the research hypothesis H_2 arguing that the variable affecting lung weakness is pollution history, and not the current level of pollution.⁸ As an additional proxy for quality of air, we also use *UrbanGreen*, i.e. square meters of green per 100 m^2 surface of urban centers in the province main city.

We control for temperature in the specification with a dummy taking value one if the three days moving average of minimum temperature was higher than 12 °C (*HighTemperature*), considering the 3-day lag of the variable to take into account the time between a possible effect and the illness onset.⁹ The reason why we control for this factor is that previous studies have shown that virus outbreaks are significantly reduced by high temperature (Lowen et al., 2007; Barreca and Shimshack, 2012; Shaman and Kohn, 2009; Zuk et al. 2009)¹⁰.

We also introduce a variable measuring the share of artisan firms at province level (*Artisan*), in order to account for potential association between pre-virus levels of intensity of local small business activity and COVID-19 outcomes. Small business employers and entrepreneurs live in a competitive environment with reduced social protection in Italy. In most cases they are suppliers of large companies in relationships where they have lower bargaining power that translates into worse trade credit conditions. Moreover, micro and artisan firms are in a higher proportion in the manufacturing sector, with reduced opportunity to convert their activities to smart working. Hence, small businesses may have a relatively lower propensity to stop their operations during the epidemic for the expected higher risk of adverse economic consequences from that decision.

To measure the efficiency of the local health system (*Health_{pca}*), we

⁸ The EU identifies as dangerous for lung diseases particulate matter (PM2.5, PM10), sulphur dioxide (Sox) and nitrogen dioxide (NOx) (see European Court of Auditors, 2018). The levels of these pollutants in the air depends on the combination of activity of emission sources (house heating, transportation, sources of energy, manufacturing and agricultural activity) with weather and geographical conditions (i.e. Pianura Padana has for its geographical structure lower air circulation). The importance of polluting sources also varies significantly. When averaged at EU level house heating is by far the most important source for PM (42 percent for PM10 and 57% for PM2.5), while transportation (39 percent) and energy sources (31 percent) for sulphur dioxide. However, these shares may vary significantly in different regions. In the North of Italy house heating accounts for 37% while 17% from intensive farming (Ispra, 2018).

⁹ Results are not significantly affected either by the days of the moving average or by the lagged days considered. Results from a further investigation on delayed effects of temperature on the virus will be published in a new version of this working paper.

¹⁰ Research on past coronaviruses show that they belong to the family of “enveloped viruses” as they are surrounded by an oily coat (a lipid bilayer). Enveloped viruses are more sensitive to temperature since low temperature hardens the coat into a rubber-like state that protects the virus longer when it outside the body. Sayadi et al. (2020) show that areas at higher risk of coronavirus outbreak are those with an average temperature between 5 and 11 °C degrees. Bannister-Tyrrell et al. (2020) provide preliminary evidence that higher temperature is associated with lower incidence of COVID-19. Notari (2020) by looking at nonsynchronous data from 42 countries finds a peak of the growth rate of contagion around 7.7 ± 3.6 °C temperature. Bukhari and Jameel (2020) show that 90 percent of cases until March 22, 2020 have been recorded in the 3–17°C temperature range and in the 3–9 g/m^3 humidity range. The authors emphasize how virus diffusion in warmer and more humid areas (regions of the United States such as Texas, New Mexico and Arizona, Asian countries such as Malaysia and Thailand and Middle East countries such as Saudi Arabia), while stronger in others with colder and drier climate (Iran, South Korea, New York and Washington).

extract the first factor from a principal component analysis which includes the number of many different medical devices (i.e. the number of lung ventilators, diving chambers, ecographs, computed tomography scanners, hemodialysis machines, medical monitors, nuclear magnetic resonance tomographs, operating rooms, radiology devices, portable radiology devices, linear particle accelerators, remote control radiology tables, immune-based automatic analyzers, computerized gamma cameras), anesthetic machines, surgical lighthead, automatic coulter counters) per 1,000 inhabitants.

As additional controls, we use population density, average household disposable income and the share of individuals aged over 65 (*Over65*), both per 1,000 inhabitants. In an alternative specification, we also include the share of Chinese residents to the total number of immigrants at the province level.

Another important proxy for contagion power concerns the speed and the amount of individual movements. We therefore include among controls a measure of internal commuting flow (*InternalCommuting*), which is calculated with Census data movement within province i , as well as a measure of imported commuting flow (*ExternalCommuting*) with Census data movements into province i from other provinces (both variables are computed per 1,000 inhabitants). We also include another proxy for the frequency of human contacts, i.e. the number of passengers on public transport divided by the total number of residents in the province (*PublicTransportUse*) and multiplied by 1,000.

Standard errors are clustered at regional level in order to account for error correlation within the region where our unit of observation (province) is located. Further details on the construction of all the variables are in Table 2.

4. Empirical findings

Summary descriptive findings of the variables used in our specification are presented in Table 3.

The first model we estimate implements maximum likelihood estimators for the parameters of a linear cross-section spatial-autoregressive model with spatial-autoregressive disturbances (SAC).¹¹ More specifically, we estimate the following equation:

$$CV19 - Outcome_i = \alpha_0 + \lambda \sum_{i \neq j} w_{ij} CV19 - Outcome_j + \sum_r \alpha_r X_i + u_i \quad \text{Eq.2}$$

where the dependent variable is the cumulative (contagion or death) outcome at a given date, X are the controls described in Eq.1, and w_{ij} coefficients are the inverse distance spatial-weighting elements using province latitude and longitude, for each of the n provinces i and j ; u_i are modelled as $u_i = \rho \sum_{i \neq j} w_{ij} + \varepsilon_i$.

SAC cross-sections estimates take a snapshot of the phenomenon at the beginning and at the end of our sample period and using as dependent variable the cumulative number of contagions (Table 4) and deaths (Table 5).

Results show that economic activity and quality of air are significantly (and consistently across model specifications) correlated with the COVID-19 outcomes. More specifically, provinces with high levels of PM10 (Tables 4 and 5, Column 1) or PM2.5 (Tables 4 and 5, Column 2), as well as with high economic activity tend to have also worse outcomes in terms of contagion and deceases; density of urban green is significantly and negatively correlated with mortality. Results for NO_2 are similar to those for PM, though with higher p-values in the estimates with contagion as dependent variable.

In order to exploit the time dimension of the data, we first perform a pooled OLS estimate including also the time trend (and its square). The dependent variable is now the daily number of new cases or deaths

¹¹ All results are confirmed also in less strict OLS models that do not account for spatial autocorrelation (available upon request).

Table 2
Variable legend.

Dependent variables	Description
Cases_pc	Cumulative number of COVID-19 daily cases over 2018 population (at province level), per 1,000 inhabitants.
New_cases_pc	Number of daily new COVID-19 daily cases over 2018 population (at province level), per 1,000 inhabitants.
Deaths_pc	Cumulative number of daily deaths over 2018 population (at province level), per 1,000 inhabitants.
New_deaths_pc	Average number of daily new deaths over 2018 population (at province level), per 1,000 inhabitants.
Day	Number of days since the first case was detected (February 24, 2020).
Lockdown	Dummy = 1 if the province was on full lockdown (as for Table 1).
PM10	Average of yearly mean values in mg/mc registered by city monitoring posts in the i-th province (Ispira, 2018), and aggregated at province level by weighing observations by the population size of the municipality where the monitoring post is located.
PM2.5	Average of yearly mean values in mg/mc registered by city monitoring posts in the i-th province (Ispira, 2018) and aggregated at province level by weighing observations by the population size of the municipality where the monitoring post is located.
NO2	Average of yearly mean values in mg/mc registered by city monitoring posts in the i-th province (Ispira, 2018) and aggregated at province level by weighing observations by the population size of the municipality where the monitoring post is located.
Urban green	Square meters of green per 100 m ² of surface area of urban centers (BES, 2016).
High temperature	Dummy = 1 if the three days moving average of minimum temperature was higher than 12 °C.
Density	Population density in the province (number of residents in 2018 in the province divided by province area)
Over65	Number of residents aged 65+ over 2018 population (at province level), per 1,000 inhabitants.
Income	Average household disposable income in the province.
Health (pca)	First factor extracted from a principal component analysis which includes the number of the following medical devices (i. e. the number of lung ventilators, diving chambers, ecographs, computed tomography scanners, hemodialysis machines, medical monitors, nuclear magnetic resonance tomographs, operating rooms, radiology devices, portable radiology devices, linear particle accelerators, remote control radiology tables, immune-based automatic analysers, computerized gamma cameras, anesthetic machines, surgical lightheads, automatic couler counters, per 1,000 inhabitants.
Public transport use	Number of people using public transports per 1,000 inhabitants.
Internal commuting	Total (work and education) internal commuting flows in the i-th province (Census data, ISTAT).
External commuting	Total (work and education) commuting flows in the i-th province from other provinces (Census data, ISTAT).
Day	Days since first case detected in Italy (February 24, 2020).
Artisan	Percent of micro (artisan) firms on total enterprises (Unioncamere-Movimprese, 2017).

alternatively. Regressors include a linear and a quadratic time trend (*Day* and *Day*²). Findings (Table 6) reveal that the COVID-19 outcomes follow an inverse U-shape exponential dynamic (the *Day*² variable is negative and significant). As in the previous estimates, other significant variables are exposure to particulate matter and the share of artisan firms. In some specifications, the share of over-65 individuals is negatively correlated with contagion, yet not with mortality. This could be explained by the fact that this age class might have responded more quickly to the restrictions and/or by the advices provided by central and local authorities. In terms of magnitude, coefficients from pooled estimates are broadly consistent with those from cross-section estimates implying a difference from the highest to the lowest PM province of 2940 contagions and 1361 deaths per month per million inhabitants for PM10, and a difference of 3160 contagions and 1456 deaths per month

per million inhabitants for PM2.5.¹²

The second panel-data approach rests on SAC fixed-effect model. In these models, province time-invariant characteristics are absorbed in the intercept. This is, however, an important feature since it allows us to partial out heterogeneous omitted factors such as industry characteristics or structural differences in regional health policies (i.e. prevalence of elders in nursing homes) that might be correlated with the dynamics of contagion and mortality. We therefore test whether the above-mentioned province-specific fixed characteristics differentially affect the *trend* of contagion and mortality in our provinces. To this purpose, we interact the time-trend variable (*day*) with each time-invariant control included in Eq.1.

Results are reported in Table 7. The role of pollution (PM10, PM2.5 or NO2) is confirmed also under this stricter analysis. More specifically, this interaction captures separately the “slope” effect on COVID-19 outcomes of the variables measuring pre-virus quality of air; in other terms, it measures the differential trends of contagion and mortality by levels of pollution. Note that the average effects are absorbed into the intercept and not identifiable in this kind of estimates. Results suggest that – net of all other province time-invariant factors – contagion and mortality tend to grow more rapidly in provinces that were highly polluted before the outbreak of COVID-19.

Overall, our empirical findings show a negative and significant correlation between pollution and both the COVID-19 outcomes under scrutiny. Moreover, the share of artisan firms has a positive and significant effect on both dependent variables. As argued above, our interpretation to this result (consistent with anecdotal evidence¹³) is that micro-firms are the most fragile part of the productive environment and therefore less likely to stop down after the beginning of the epidemic to avoid the risk of default. Moreover, a higher proportion of them operates in the manufacturing industry and have relatively lower chances to shift to smart working during the epidemic. We cannot however exclude that the positive and significant coefficient of the artisan variable conceals the effect of different dynamics of human interactions at province level during the estimation period, which are typical of areas with higher economic activity, and therefore correlated with the spread of the virus.

As a final test, we assess the relative role of the presence of the Chinese community in the spread of the disease. In the pooled regressions of contagion (Table 6), we also include among regressors the share of Chinese immigrants to total population at the province level. The coefficient is negative and not statistically significant, with $\beta = -0.0659$ and $p = 0.544$ in the estimate with PM10, $\beta = -0.698$ and $p = 0.597$ in the estimate with PM2.5, and $\beta = -0.0491$ and $p = 0.566$ in the estimate with NO2 (available upon request).

5. Lockdown and mortality

In this section, we take into account the correlation between

¹² Our model outperforms the purely autoregressive model that include among regressors only time trends ($R^2 = 0.105$ vs $R^2 = 0.271$ for PM10, $R^2 = 0.265$ for PM2.5, and $R^2 = 0.277$ for NO2). The differences in the goodness of fit and the significance of our regressors are similar when we consider a cubic trend model, which captures the convexity of the initial increasing trend. Results are available upon request.

¹³ A well-known case here is that of Arzano Lombardo where at end February appeared the first contagion cases in the province of Bergamo. Due to the strong relevance in terms of small-medium business the authorities decided not to create a red zone there, differently from what happened in Codogno. The outcome has been a strong diffusion of contagion and a number of deaths largely exceeding those of the previous year in the same month (100 against 10). Beyond authorities' decision we interpret the significance of this variable as the push from small corporate owners not to close their activities due to the fear of default and the effect of this decision on the number of adverse COVID-19 outcomes (<https://www.ilpost.it/2020/04/01/disastro-alzano-lombardo-nembro/>).

Table 3
Summary statistics.

Variable		Mean	Std. Dev.	Min	Max	Observations
Cases_pc	overall	1.196	1.951	0	14.810	N = 5,081
	between		1.362	0.076	7.244	n = 96
	within		1.404	-5.901	8.762	T = 52.927
New_cases_pc	overall	0.056	0.093	-0.672	1.708	N = 5,081
	between		0.053	0.004	0.279	n = 96
	within		0.077	-0.671	1.709	T = 52.927
New_deaths_pc	overall	0.021	0.028	0	0.209	N = 3,570
	between		0.024	0.001	0.112	n = 92
	within		0.015	-0.072	0.123	T = 38.804
Deaths_pc	overall	0.434	0.631	0	4.480	N = 3,152
	between		0.449	0	2.043	n = 85
	within		0.443	-1.479	2.963	T = 37.082
PM10	overall	24.416	5.238	13.164	35.509	N = 5,081
	between		5.267	13.164	35.509	n = 96
	within		0.000	24.416	24.416	T = 52.927
PM2.5	overall	15.455	4.526	5.450	26.423	N = 4,763
	between		4.548	5.450	26.423	n = 90
	within		0.000	15.455	15.455	T = 52.922
NO2	overall	23.851	7.998	3.000	47.090	N = 5,028
	between		8.037	3.000	47.090	n = 95
	within		0.000	23.851	23.851	T = 52.926
Urban green	overall	1.796	2.869	0.100	19.500	N = 5,081
	between		2.884	0.100	19.500	n = 96
	within		0.000	1.796	1.796	T = 52.927
Day	overall	26.973	15.288	1	53	N = 5,081
	between		0.306	24	27.038	n = 96
	within		15.285	0.934	53.973	T = 52.927
High temperature	overall	0.030	0.170	0	1	N = 5,081
	between		0.103	0	0.774	n = 96
	within		0.136	-0.744	1.011	T = 52.927
Density	overall	262.084	350.217	37.166	2623.520	N = 5,081
	between		351.788	37.166	2623.520	n = 96
	within		0.000	262.084	262.084	T = 52.927
Over65	overall	235.746	24.052	173.927	290.665	N = 5,081
	between		24.190	173.927	290.665	n = 96
	within		0.000	235.746	235.746	T = 52.927
Income	overall	0.109	0.070	0.011	0.406	N = 5,081
	between		0.070	0.011	0.406	n = 96
	within		0.000	0.109	0.109	T = 52.927
Health (pca)	overall	0.233	2.683	-5.006	9.682	N = 5,081
	between		2.695	-5.006	9.682	n = 96
	within		0.000	0.233	0.233	T = 52.927
Public transport use	overall	0.171	0.193	0.010	1.397	N = 5,081
	between		0.194	0.010	1.397	n = 96
	within		0.000	0.171	0.171	T = 52.927
Internal commuting	overall	0.432	0.049	0.286	0.577	N = 5,081
	between		0.049	0.286	0.577	n = 96
	within		0.000	0.432	0.432	T = 52.927
External commuting	overall	0.035	0.021	0.004	0.113	N = 5,081
	between		0.021	0.004	0.113	n = 96
	within		0.000	0.035	0.035	T = 52.927
Artisan	overall	0.267	0.061	0.118	0.382	N = 5,081
	between		0.061	0.118	0.382	n = 96
	within		0.000	0.267	0.267	T = 52.927

lockdown decisions and COVID-19 related outcomes (research hypothesis H_1). It has to be noticed here that correlation does not imply causation, yet a perfectly randomized experiment – as discussed in section 7 – is not feasible in the present context. A second-best approach rests on a reasonable approximation to this counterfactual, which could be done in several ways, e.g. by building synthetic controls or by exploiting out-of-sample predictions from (in-sample) pre-lockdown estimated parameters. Synthetic controls might be difficult to be built here since one has to exploit post-lockdown trends of regions that are most similar the Italian ones in many dimensions (e.g. institutional arrangements, cultural background, economic conditions, etc.). Other EU regions could be natural candidates, yet Italy was the first in implementing social-distancing measures, while other countries did it later and in different ways, thereby making it hard to obtain good matches on pre-lockdown characteristics.

We therefore follow the second approach and construct a counter-

factual trend through out-of-sample predictions. This approach seems particularly advisable given that epidemiologic dynamics are often modelled using deterministic approaches.¹⁴ More specifically, we first estimate the following equation:

$$Mortality_{mt} = \gamma_0 + \gamma_1 Day_{mt} + \gamma_2 Day_{mt}^2 + \gamma_3 Cases_{it-4} + \eta_{mt} \quad Eq.3$$

where *Mortality* is the number of deaths per 1,000 inhabitants in day *t* and municipality *m*, and *Cases* is the one week (4-day) lagged number of positive cases per 1,000 inhabitants in province *i* (where municipality *m*

¹⁴ Given the small share of population contagions during the estimation period (far lower than 10 percent even with the less conservative forecast applying an exogenous fixed 2 percent mortality rate) we may reasonably assume that we are far from the herd immunity, and therefore our deterministic model continues to be valid to predict the counterfactual in this time period.

Table 4
Major factors explaining variation in COVID-19 contagion (cross-section).

	(1)	(2)	(3)	(4)	(5)	(6)
	As of March 5th, 2020			As of April 17th, 2020		
PM10	0.0217*** (0.00705)			0.152*** (0.0464)		
PM2.5		0.0249** (0.00993)			0.185*** (0.0690)	
NO2			0.00894* (0.00537)			0.0442 (0.0324)
Urban green	−0.00898 (0.0109)	−0.0143 (0.0131)	−0.00745 (0.0113)	−0.0464 (0.0688)	−0.0915 (0.0874)	−0.0285 (0.0715)
High temperature	−0.117 (0.181)	−0.0578 (0.189)	−0.128 (0.190)	0.256 (0.523)	0.466 (0.602)	0.197 (0.560)
Density	−7.19e-05 (0.000102)	−4.58e-05 (0.000107)	−0.000141 (0.000115)	−0.000478 (0.000663)	−0.000116 (0.000741)	−0.00102 (0.000706)
Over65	−0.00379** (0.00177)	−0.00486** (0.00190)	−0.00437** (0.00185)	−0.00998 (0.0109)	−0.0201* (0.0117)	−0.0157 (0.0113)
Income	0.580 (0.543)	0.731 (0.638)	0.366 (0.564)	9.377*** (3.241)	10.64*** (3.785)	8.227** (3.450)
Health (pca)	0.00352 (0.0142)	0.00984 (0.0166)	−1.77e-05 (0.0148)	−0.0812 (0.0851)	−0.000575 (0.100)	−0.101 (0.0916)
Public transport use	0.140 (0.180)	0.105 (0.186)	0.0567 (0.184)	−0.206 (1.140)	−0.373 (1.194)	−0.769 (1.148)
Internal commuting	−1.822** (0.811)	−2.188** (0.892)	−1.839** (0.861)	6.081 (4.750)	3.102 (5.394)	8.293* (4.933)
External commuting	0.997 (1.920)	0.800 (2.078)	2.850 (1.897)	−9.006 (11.81)	−13.86 (13.47)	6.843 (11.13)
Artisan	2.023*** (0.730)	1.847** (0.808)	1.862** (0.784)	26.74*** (4.567)	25.95*** (5.107)	25.26*** (4.658)
Constant	0.612 (0.530)	1.223** (0.560)	1.099** (0.535)	−10.08*** (3.182)	−5.057 (3.512)	−7.457** (3.322)
λ	0.0781 (0.546)	0.00886 (0.562)	0.117 (0.570)	0.457* (0.237)	0.369 (0.290)	0.659*** (0.203)
ρ	0.225 (0.592)	0.355 (0.515)	0.343 (0.547)	−2.158*** (0.759)	−1.700* (0.889)	−2.386*** (0.793)
σ^2	0.0840*** (0.0121)	0.0912*** (0.0136)	0.0904*** (0.0131)	2.985*** (0.467)	3.299*** (0.532)	3.211*** (0.512)
Observations	96	90	95	95	89	94

Cross-sectional SAC model. Columns 1–3 refer to March 5th, 2020 and columns 4–6 refer to April 17th, 2020; ρ and λ are spatial autoregressive parameters measuring the degree of spatial correlation in the number of new cases and the disturbance term respectively; σ^2 is the Maximum Likelihood residuals variance. Standard errors are clustered at regional level, *** $p < 0.01$, ** $p < 0.05$, * $p < 0.1$.

is located).¹⁵ Notice that here we use data at the municipality level, which is the smallest Italian geographic unit —mortality is the only COVID-19 related outcome available at such a geographic level. We perform an OLS fixed effects panel regression,¹⁶ clustering standard errors at regional level to account for intra-regional error correlation. Hence, we extract the predicted values $T_Mortality_{mt}$, which capture our “real” mortality trend. As argued above, fixed-effects panel models have the advantage of partialling out time-invariant unobserved factors that might explain different trends of contagion and mortality across municipalities such as quality of local health system, number of elderly individuals in nursing homes and human mobility.

To build a “counterfactual” trend, we re-estimate Eq. 3 by restricting the sample to $t \leq l$, where l is March 12th, 2020, i.e. the day after full lockdown is introduced in the entire country. Hence, we compute the predicted values also for $t > l$, which provide us with the out-of-sample linear prediction of the post-lockdown mortality trend, i.e.

$C_Mortality_{mt}$. The latter can be thought of an approximation to the counterfactual trend of mortality, which describes how mortality would have evolved over time had lockdown not been introduced.

Fig. 2 shows the two trends averaged across municipalities. This figure highlights that the two trends start diverging significantly from March 20th, 2020, i.e. 8 days after full lockdown, when the real mortality trend began to decrease slightly. To further evaluate whether the two trends are statistically different after March 12th, 2020 we first compute their difference as $Mortality_diff_{mt} = C_Mortality_{mt} - T_Mortality_{mt}$ and regress it through fixed-effects OLS on a series of time dummies. Estimated marginal means from this regression are plotted in Fig. 3 and confirm the previous findings, with the gap between counterfactual and real mortality trend starting to increase after lockdown.

To assess the role of past exposure to pollution, we perform OLS fixed-effects regressions of $Mortality_diff_{mt}$ on lockdown decisions, and interact the latter with PM2.5, PM10 and NO2. More specifically, we introduce a dummy variable equal to one if the municipality is in a province with average concentration of PM2.5 (or, in a separate model, PM10 or NO2) in 2018 equal or above their sample mean, and zero otherwise. As for lockdown, we create a dummy variable ($Lockdown_{it}$) equal to one if the municipality m in province i in day t was under the

¹⁵ Although the time window from illness onset to death is larger, we set it at 4 to maximize the number of time periods in the sample. The inclusion of high order lags reduces the number of observed time periods, thereby hindering the goodness of fit, especially for the prediction of the counterfactual trend (which is based on fewer time periods).

¹⁶ We decided to opt for OLS fixed-effects regressions since they seem to perform better in terms of AIC and BIC criteria than Poisson fixed-effects ones. Under the same criteria, the chosen specification also outperforms other specifications that instead use the number of deaths (and cases) or their log.

Table 5
Major factors explaining variation in mortality (cross-section).

	(1)	(2)	(3)	(4)	(5)	(6)
	As of March 5th, 2020			As of April 15th, 2020		
PM10	0.000856** (0.000333)			0.00109*** (0.000297)		
PM2.5		0.00152*** (0.000464)			0.00153*** (0.000398)	
NO2			0.000643*** (0.000244)			0.000463** (0.000217)
Urban green	−0.000490 (0.000507)	−0.000521 (0.000584)	−0.000307 (0.000520)	−0.000384 (0.000467)	−0.000523 (0.000531)	−0.000177 (0.000494)
High temperature	−0.00241 (0.00854)	−0.00111 (0.00852)	−0.00599 (0.00889)	−0.00367 (0.00494)	−0.000387 (0.00534)	−0.00348 (0.00500)
Density	−2.02e-06 (4.76e-06)	−1.96e-06 (4.79e-06)	−7.57e-06 (5.23e-06)	−3.44e-06 (4.29e-06)	−2.27e-06 (4.32e-06)	−6.01e-06 (4.71e-06)
Over65	0.000132 (8.47e-05)	8.67e-05 (8.62e-05)	0.000112 (8.41e-05)	0.000142* (7.49e-05)	6.22e-05 (8.13e-05)	0.000139* (7.82e-05)
Income	0.0138 (0.0253)	0.0307 (0.0288)	0.0160 (0.0257)	0.0180 (0.0225)	0.0440* (0.0260)	0.0161 (0.0232)
Health (pca)	0.000712 (0.000669)	0.000824 (0.000748)	0.000601 (0.000680)	0.000149 (0.000597)	0.000884 (0.000672)	−0.000331 (0.000635)
Public transport use	−0.00349 (0.00853)	−0.00274 (0.00842)	−0.00715 (0.00844)	−0.0167** (0.00770)	−0.0177** (0.00772)	−0.0225*** (0.00769)
Internal commuting	−0.0324 (0.0382)	−0.0524 (0.0404)	−0.0452 (0.0392)	−0.0236 (0.0342)	−0.0545 (0.0355)	−0.0139 (0.0336)
External commuting	−0.0673 (0.0905)	−0.111 (0.0938)	−8.30e-05 (0.0858)	−0.0315 (0.0808)	−0.0705 (0.0849)	0.0250 (0.0783)
Artisan	0.0866** (0.0343)	0.0553 (0.0363)	0.0679** (0.0346)	0.125*** (0.0305)	0.102*** (0.0326)	0.124*** (0.0322)
Constant	−0.0382 (0.0313)	−0.00552 (0.0316)	−0.0225 (0.0276)	−0.0613** (0.0242)	−0.0162 (0.0286)	−0.0514** (0.0245)
λ	0.371 (0.536)	0.155 (0.521)	0.504 (0.443)	0.241 (0.481)	0.0510 (0.576)	0.334 (0.403)
ρ	0.102 (0.708)	0.457 (0.451)	−0.371 (0.856)	−0.613 (0.814)	−0.159 (0.751)	−1.364 (0.906)
σ^2	0.000186*** (2.69e-05)	0.000186*** (2.78e-05)	0.000186*** (2.73e-05)	0.000146*** (2.13e-05)	0.000147*** (2.19e-05)	0.000152*** (2.29e-05)
Observations	96	90	95	96	90	95

Cross-sectional SAC model. Columns 1–3 refer to March 5th, 2020 and columns 4–6 refer to April 15th, 2020; ρ and λ are spatial autoregressive parameters measuring the degree of spatial correlation in the number of new deaths and the disturbance term, respectively; σ^2 is the Maximum Likelihood residuals variance. Standard errors are clustered at regional level, *** $p < 0.01$, ** $p < 0.05$, * $p < 0.1$.

total block, and zero otherwise.¹⁷ In alternative specifications, we also consider a different definition of lockdown by including an indicator (*After_12/3*) for $t > l$. Regression results are reported in Table 7. The positive and significant coefficient of the lockdown indicators suggest that mortality would have been larger if lockdown decisions were not implemented. The lockdown effects range from about −0.12 to −0.15 percentage points (Table 7, column 1 and 4). Hence, our estimates suggest that lockdown decisions are on average associated with a decline in the number of deaths per 1,000 inhabitants by 80–100 percent if we consider the sample mean of the overall predicted mortality (i.e. 0.15), which includes both $C_Mortality_{mt}$ and $T_Mortality_{mt}$.

Importantly, the positive association between lockdown and mortality is larger in less polluted areas as documented by the significant interaction between lockdown and the pollution variables (Table 8, columns 2–3 and 5–6). The positive coefficient of the interaction, if interpreted jointly with the trends plotted in Fig. 4, suggests that without lockdown mortality would have grown more in the highly polluted cities.

As a final check for the joint role of lockdown decisions and pollution in mortality, we replicate this analysis by duplicating the municipalities in our sample. The artefactually “cloned” observations take on the

previously estimated *counterfactual* trend in mortality ($C_Mortality_{mt}$), whereas the original observations take on the *real* trend in mortality ($T_Mortality_{mt}$). By doing so, we artificially create two groups of municipalities, namely the “treated” municipalities, i.e. those with the real predicted trend, and the “control” municipalities, i.e. those with the predicted counterfactual trend. Of course, the latter is a “synthetic” control since observations with a counterfactual trend do not really exist; in facts, they have been imputed by duplicating the observations in our sample and assigning them the values of the counterfactual estimated trend. This trick should deliver the same results as the previous ones, while providing us at the same time with a quasi-experimental sample on which we could implement the Differences-in-Differences approach (DiD).

Hence, we create a *treatment* indicator ($Real_trend_m$) which is equal to one for municipalities with the *real* mortality trend, and zero for their “clones” receiving the counterfactual trend. Figure A1 in the appendix reports estimated margins from a regression of the overall mortality trend, i.e. $Mortality_{mt}$, on time dummies and their interaction with the treatment indicator ($Real_trend_m$). As expected, the two trends mirror those plotted in Fig. 2, with the real trend in mortality decreasing after about a week from the day when full lockdown was introduced in the country.

To obtain DiD estimates, we regress the overall mortality trend on our treatment indicator ($Real_trend_m$), our *post-treatment* indicator, i.e. the lockdown dummy ($Lockdown_{it}$ or *After_12/3*), and the interactions between these two variables. In augmented models we also interact

¹⁷ The total lockdown decision was taken on the 8th of March in Lombardia and 18 provinces of Piemonte, Emilia Romagna and Marche, while on the 10th of March it was extended to the rest of Italy (see Table 1). We consider March 10th as the decree has been issued on the evening of March 9th and, therefore, it has been operating since March 10th.

Table 6

Major factors explaining variation in COVID-19 contagion (pooled).

Dep. Var.:	(1)	(2)	(3)	(4)	(5)	(6)
	<i>New_cases_pc</i>	<i>New_cases_pc</i>		<i>New_deaths_pc</i>	<i>New_deaths_pc</i>	
Day	0.0105*** (0.00222)	0.0110*** (0.00225)	0.0105*** (0.00222)	0.00369** (0.00131)	0.00385** (0.00138)	0.00363** (0.00133)
Day ²	−8.89e-05*** (2.11e-05)	−9.38e-05*** (2.16e-05)	−9.01e-05*** (2.09e-05)	−3.77e-05*** (1.27e-05)	−3.92e-05*** (1.34e-05)	−3.71e-05*** (1.29e-05)
PM10	0.00352** (0.00162)			0.00162** (0.000634)		
PM2.5		0.00458** (0.00209)			0.00211** (0.000925)	
NO2			0.00181*** (0.000608)			0.000867*** (0.000280)
Urban green	−0.00166 (0.00117)	−0.00279*** (0.000835)	−0.00121 (0.00131)	−0.000686 (0.000482)	−0.00116** (0.000441)	−0.000494 (0.000561)
High temperature	−0.00882 (0.00578)	−0.00286 (0.00659)	−0.0156*** (0.00452)	0.000367 (0.00147)	0.00382** (0.00154)	−0.00305 (0.00376)
Density	4.61e-06 (7.01e-06)	8.70e-06 (5.70e-06)	−1.06e-05 (9.55e-06)	−2.73e-06 (4.36e-06)	−1.63e-06 (3.86e-06)	−9.48e-06 (5.81e-06)
Over65	−0.000336 (0.000196)	−0.000523** (0.000234)	−0.000448* (0.000229)	1.42e-05 (0.000122)	−4.51e-05 (0.000136)	−2.02e-05 (0.000136)
Income	0.145** (0.0592)	0.180** (0.0679)	0.123** (0.0553)	0.0241 (0.0188)	0.0256 (0.0290)	0.0158 (0.0148)
Health (pca)	−0.000960 (0.00177)	0.000392 (0.00169)	−0.00151 (0.00168)	−1.93e-05 (0.000515)	0.000187 (0.000571)	−0.000350 (0.000533)
Public transport use	0.0155 (0.0152)	0.00875 (0.0144)	0.00270 (0.0209)	−0.0134 (0.00801)	−0.0165** (0.00729)	−0.0201*** (0.00669)
Internal commuting	0.0697 (0.104)	−0.00626 (0.0926)	0.0650 (0.0840)	−0.0332 (0.0427)	−0.0575 (0.0406)	−0.0358 (0.0425)
External commuting	−0.221 (0.195)	−0.338** (0.142)	0.0855 (0.215)	−0.0506 (0.0838)	−0.0920 (0.0701)	0.0754 (0.0879)
Artisan	0.561*** (0.0875)	0.520*** (0.0798)	0.523*** (0.0894)	0.202*** (0.0646)	0.180*** (0.0540)	0.185** (0.0679)
Constant	−0.420*** (0.0670)	−0.328*** (0.0544)	−0.342*** (0.0500)	−0.125*** (0.0355)	−0.0890*** (0.0283)	−0.0917*** (0.0224)
Observations	5081	4763	5028	4992	4680	4940
R-squared	0.271	0.265	0.277	0.318	0.308	0.293

Pooled OLS model. Standard errors are clustered at regional level, ***p < 0.01, **p < 0.05, *p < 0.1.

these two indicators with the aforementioned pollution dummies for PM10, PM2.5 or NO2. Results are reported in Appendix, Table A1. Consistent with previous results, lockdown seems effective in reducing mortality as shown by our DiD coefficient, i.e. the negative and significant interaction between treatment and post-treatment indicator in column 1 ($Lockdown_{it} * Real_trend_m$) or 4 ($After_12/3_t * Real_trend_m$).

The interpretation of the results with the triple interaction including the pollution indicator (columns 3 and 6) is slightly more complicated. For this reason, we plot the estimated margins (Figure A2 in Appendix), which overall suggest that the adverse effects of COVID-19 on mortality would have been harsher without lockdown, especially in highly polluted provinces.

Three main robustness checks have been implemented by augmenting Eq. 3 with other covariates capturing the potential unobserved heterogeneity in the level of economic activity, the quality of the health system and mobility patterns. First, we include to the baseline model described in Eq. 3, two interaction terms, i.e. between the time-varying lagged contagion ($Cases_{it-4}$) and i) the share of micro-enterprises in the province ($Artisan_{it}$), and ii) the normalized first extracted component from a principal component analysis including our three human mobility proxies measured at the province level, i.e. $InternalCommuting_{it}$, $ExternalCommuting_{it}$, and $PublicTransportUse_{it}$. These interactions allow us to mitigate unobserved heterogeneity that could be induced by time-variant behavior of firms and individuals in complying with lockdown decisions. The underlying assumption behind the choice of these variables is that the likelihood of incompliance would be higher in provinces with a high fraction of firms that cannot easily adopt smart-work solutions as well as in provinces characterized by large human mobility.

In the second alternative specification, we include the interaction between $Cases_{it-4}$ and the aforementioned proxy for efficiency of the

local health system ($Health_{pca}$), jointly with the interaction between $Cases_{it-4}$ and the first extracted factor human mobility component introduced above. These new interactions should capture the differential role pre-virus mobility and health system efficiency may have played in mortality for areas with high vs. low levels of contagion.

In the third model specification, relying on Pepe et al. (2020), we introduce a time-varying variable named “potential encounter network”, which is a proxy for the average contact rate (at the province level), or the number of unique contacts made by a person on a typical day.¹⁸ The inclusion of this variable should account for (time-varying) unobserved differences in compliance with lockdown and social distancing measures across Italian provinces, which might affect the geographic distribution of mortality over time. In addition to this variable, we include the interaction between the time trend (and its square) and $Health_{pca}$ also in this model. To control for differences across

¹⁸ This variable has been computed by the authors exploiting daily geocoded data at province level on individuals' mobility in order to create a time-varying proximity network among users based on time and location of their visits. The mobility data used by Pepe et al. (2020) are based on Cuebiq, a location intelligence, and measurement platform. We used the variable named “time series of the daily average degree of the potential encounter network”, which has been made available by the authors here: <https://data.humdata.org/dataset/covid-19-mobility-italy>. The time series of individual mobility patterns is available from Feb. 7th 2020 to March 21st 2020. When we matched this variable with our mortality data, we imputed missing values for the period March 21st – April 15th with the individual mobility patterns as averaged across March 15th and March 21st, assuming that – during the lockdown period – mobility after March 21st was similar to mobility as measured few days before that date.

Table 7Major factors explaining variation in mortality and contagion (*fixed effects*).

Dep. Var.:	(1)	(2)	(3)	(4)	(5)	(6)
	<i>New_cases_pc</i>			<i>New_deaths_pc</i>		
Day	−0.0157*** (0.00388)	−0.0110*** (0.00369)	−0.00664** (0.00277)	−0.00555*** (0.000858)	−0.00365*** (0.000799)	−0.00210*** (0.000727)
Day ²	8.85e-05** (3.82e-05)	5.29e-05 (3.59e-05)	−6.87e-06 (2.52e-05)	3.29e-05*** (8.18e-06)	2.03e-05*** (7.51e-06)	3.38e-07 (6.80e-06)
Day*PM10	0.000826*** (0.000111)			0.000364*** (2.45e-05)		
Day ² *PM10	−8.42e-06*** (1.16e-06)			−3.48e-06*** (2.44e-07)		
Day*PM2.5		0.00122*** (0.000143)			0.000544*** (3.10e-05)	
Day ² *PM2.5		−1.25e-05*** (1.49e-06)			−5.29e-06*** (3.08e-07)	
Day*NO2			0.000404*** (7.02e-05)			0.000206*** (1.64e-05)
Day ² *NO2			−3.83e-06*** (7.29e-07)			−1.97e-06*** (1.64e-07)
Day*Artisan	0.0124*** (0.00177)	0.0121*** (0.00190)	0.0106*** (0.00173)	0.00220*** (0.000403)	0.00210*** (0.000427)	0.00200*** (0.000418)
Day*Urban green	−1.21e-05 (2.56e-05)	−2.45e-05 (3.01e-05)	−4.30e-06 (2.44e-05)	−1.88e-05*** (5.84e-06)	−1.89e-05*** (6.76e-06)	−1.75e-05*** (5.89e-06)
High temperature	−0.00979 (0.00872)	−0.0109 (0.00930)	−0.00700 (0.00842)	−0.00110 (0.00213)	−0.000713 (0.00224)	0.00255 (0.00221)
Day*Density	7.60e-07*** (2.41e-07)	8.02e-07*** (2.49e-07)	3.42e-07 (2.51e-07)	8.79e-08 (5.50e-08)	1.06e-07* (5.60e-08)	1.70e-08 (6.05e-08)
Day*Over65	1.25e-05*** (4.22e-06)	1.02e-05** (4.48e-06)	1.06e-05*** (4.08e-06)	1.98e-06** (9.62e-07)	8.88e-07 (1.00e-06)	2.34e-06** (9.85e-07)
Day*Income	0.00331** (0.00131)	0.00377** (0.00152)	0.00370*** (0.00124)	0.000713** (0.000299)	0.000844** (0.000342)	0.000686** (0.000300)
Day*Health (pca)	−5.50e-05 (3.42e-05)	−3.37e-05 (3.92e-05)	−5.25e-05 (3.26e-05)	−1.00e-05 (7.79e-06)	6.41e-07 (8.80e-06)	−1.59e-05** (7.86e-06)
Day*Public transport use	7.45e-05 (0.000429)	1.38e-05 (0.000437)	9.48e-05 (0.000404)	−8.82e-05 (9.77e-05)	−0.000126 (9.80e-05)	−0.000221** (9.75e-05)
Day*Internal commuting	0.00931*** (0.00197)	0.00836*** (0.00212)	0.00839*** (0.00189)	0.00169*** (0.000449)	0.00121** (0.000475)	0.00156*** (0.000457)
Day*External commuting	−0.0163*** (0.00459)	−0.0185*** (0.00490)	−0.0125*** (0.00419)	−0.00235** (0.00105)	−0.00265** (0.00110)	−0.00141 (0.00101)
ρ	−0.799*** (0.101)	−0.851*** (0.0968)	−0.349** (0.146)	−0.606*** (0.113)	−0.683*** (0.110)	−0.473*** (0.119)
λ	0.786*** (0.0295)	0.792*** (0.0281)	0.671*** (0.0575)	0.766*** (0.0325)	0.764*** (0.0312)	0.748*** (0.0371)
σ^2	0.00464*** (9.80e-05)	0.00485*** (0.000106)	0.00418*** (8.86e-05)	0.000306*** (6.22e-06)	0.000310*** (6.53e-06)	0.000309*** (6.30e-06)
Observations	4608	4320	4560	4992	4680	4940
R-squared	0.177	0.170	0.181	0.161	0.187	0.127
Number of Provinces	96	90	95	96	90	95

Panel Fixed-effects SAC model; ρ and λ are spatial autoregressive parameters measuring the degree of spatial correlation in the number of new cases or deaths and the disturbance term, respectively; σ^2 is the Maximum Likelihood residuals variance. Standard errors are clustered at regional level, ***p < 0.01, **p < 0.05, *p < 0.1.

provinces in pre-lockdown mobility patterns that could have influenced the mortality trend afterwards, we also include the interaction between the time trend (and its square) and the (time-invariant) potential encounter network *before* the outbreak of the virus. The latter is computed by averaging the potential encounter network in the time period Feb. 7th 2020–Feb. 24th 2020.

Results from all these alternative model specifications are similar to those obtained from the baseline model in Eq. 3, and are available upon request.

6. Robustness checks

Our results are robust to a series of alternative empirical strategies. First, the nature of our dependent variable, a non-negative count of a

relatively rare event, may call for a non-negative binomial regression. Results from this model are presented in Table A2 and confirm our main findings. Since we do not know the true exposed population (and we take into account the overall population in our dependent variable), we set the time dimension (i.e., the logarithm of the day variable) as our offset variable. A further investigation may look at the actual number of people tested as offset. These data are not currently available at province level, and those at regional level suffer from multiple counting because of repeated testing of positive cases.

Furthermore, since our analysis is based on daily data, two additional concerns can arise. First, provinces may differ among themselves in testing efficiency during a week. Second, there are a few provinces that have reallocated some positive cases to other provinces because of health facilities capacities or registration errors (note, however, that this

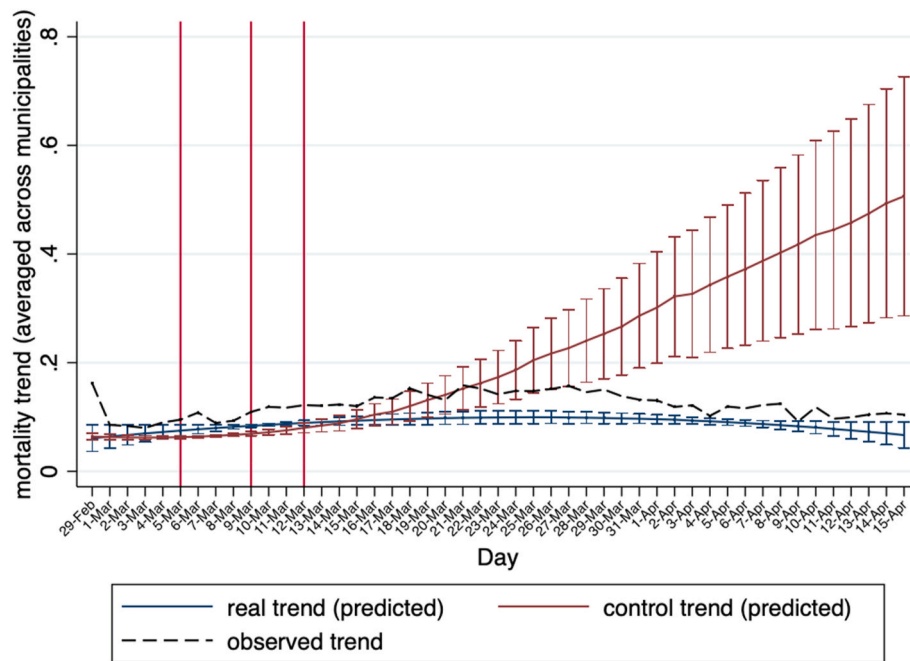


Fig. 2. COVID-19 mortality: real and counterfactual trend.

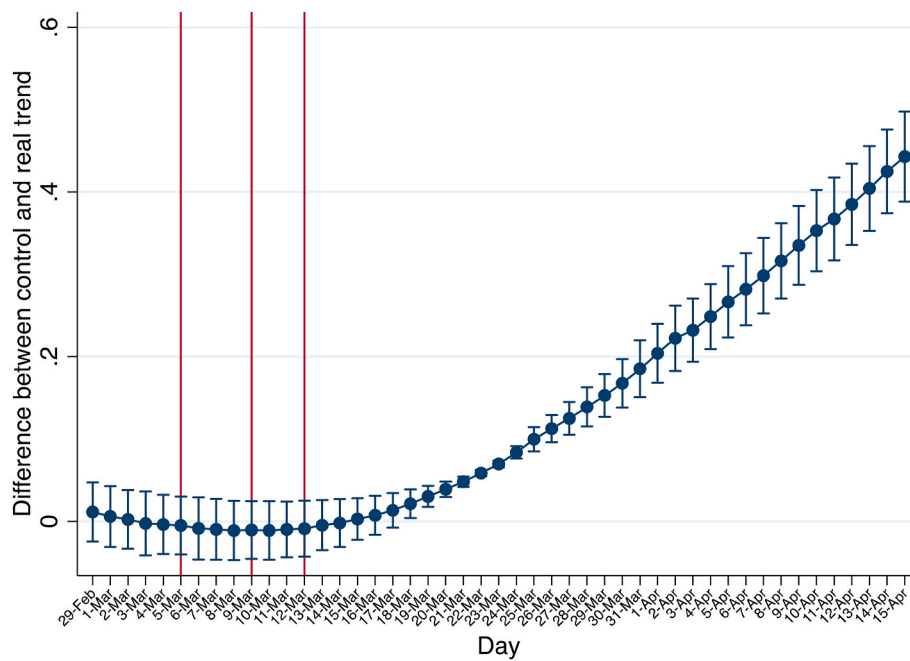


Fig. 3. COVID-19 mortality: difference between real and counterfactual trend.

problem concerns estimates on positive cases while not those on deaths). In order to address these concerns, we aggregate our data at weekly level and re-run our main estimates. In particular, we run pooled OLS and panel fixed-effects OLS models with a dummy for each week in our observed period. Table A3 and A4 in Appendix confirm our findings on the positive and significant link between the pollutant measures and our

outcome measures, as well as the presence of a non-linear time trend.

An additional possible source of bias can be introduced by potential outliers. Results could potentially be driven by a few provinces that exhibit a number of new cases or deaths that is exceptionally far from the average. In Appendix B we provide a detailed analysis of potential outliers by identifying the most “influential” provinces. However, our

Table 8The role of lockdown and pollution in reducing mortality (*fixed effects OLS*).

Dep. Var: difference in predicted mortality trends (C-R)	(1)	(2)	(3)	(4)	(5)	(6)	(7)	(8)
Lockdown	0.130*** (0.0207)	0.0918*** (0.00862)	0.100*** (0.00796)	0.101*** (0.00881)				
lockdown*PM2.5 \geq median		0.0890*** (0.0247)						
lockdown*PM10 \geq median			0.0629** (0.0286)					
lockdown*NO2 \geq median				0.0633** (0.0256)				
After 12/3					0.154*** (0.0268)	0.102*** (0.00945)	0.112*** (0.00881)	0.114*** (0.0104)
After 12/3*PM2.5 \geq median						0.110*** (0.0290)		
After 12/3*PM10 \geq median							0.0840** (0.0329)	
After 12/3*NO2 \geq median								0.0817** (0.0293)
Constant	0.00804 (0.0159)	0.00240 (0.00943)	0.00521 (0.0140)	0.00540 (0.0129)	0.000336 (0.0187)	-0.00169 (0.00997)	-0.000566 (0.0148)	-0.000571 (0.0137)
Observations	87,268	84,690	86,935	86,621	87,268	84,690	86,935	86,621
R-squared	0.147	0.164	0.155	0.155	0.246	0.279	0.265	0.264
Number of municipalities	5761	5561	5733	5704	5761	5561	5733	5704

Standard errors are clustered at regional level. Dependent variable: difference between previously estimated *counterfactual* (C) and *real* (R) trend in mortality; ***p < 0.01, **p < 0.05, *p < 0.1.

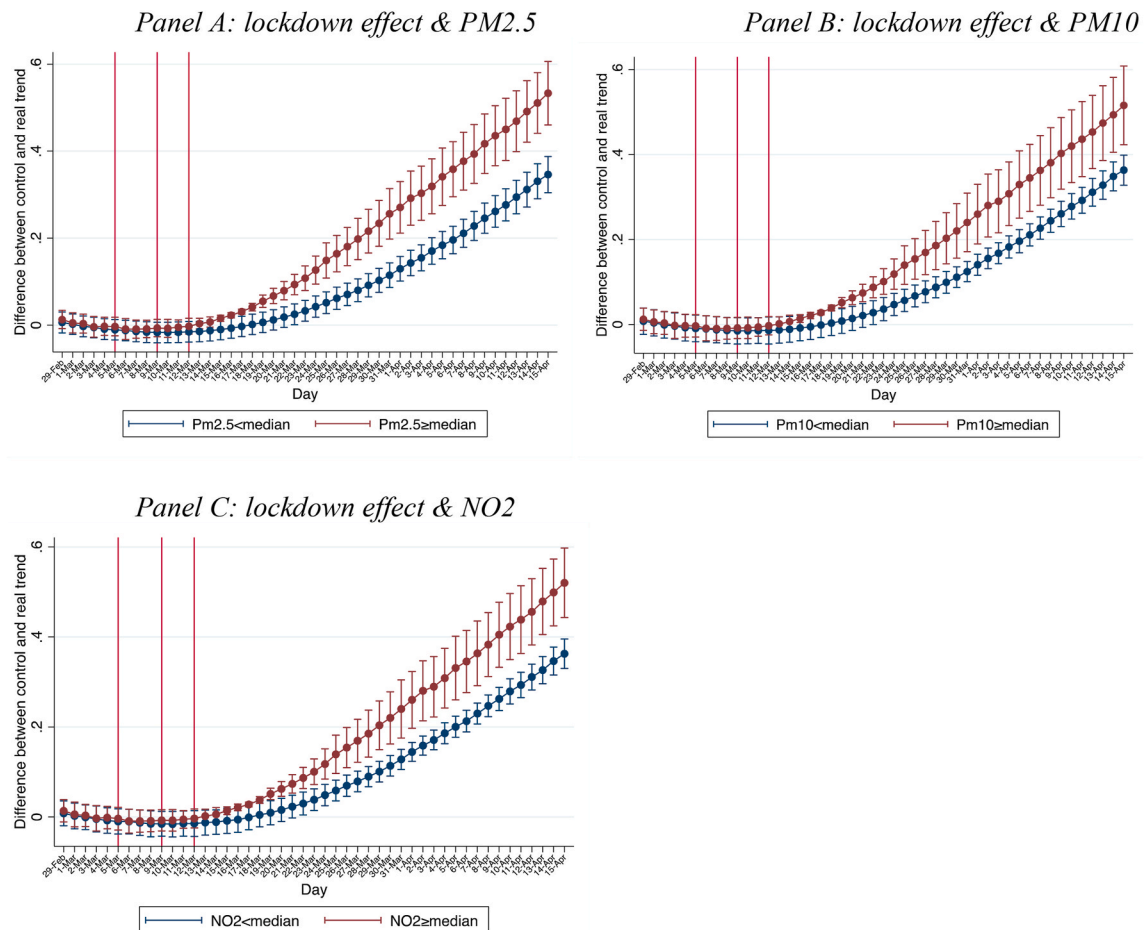


Fig. 4. The positive coefficient of the interaction, if interpreted jointly with the trends plotted in Figure 4, suggests that without lockdown mortality would have grown more in the highly polluted cities.

findings are robust to the exclusion of these provinces.

In an additional robustness check we compute the reproduction number (R_0) for each province on each day. To this purpose, we rely on the SIR (Susceptible Infected Recovered) methodology as proposed by Gu et al. (2020), and summarized by Agosto et al. (2020). The theoretical framework is based on the computation of the baseline reproduction number as $R_0 = \frac{f(1-\alpha)\mathbb{E}(T)}{h}$, where f is the probability of getting infected; $\mathbb{E}(T)$ is the mean incubation time in case of infection; h is the probability of detecting the infected cases; and α is the probability of isolating the contacts of the infected case. For the spread of COVID-19 in France, Gu et al. (2020) uses the Gamma distribution for T , with $\mathbb{E}(T) = 7.5$ (based on contagion data from China), and simulate how R_0 changes in response to different values of α and h . Since such a simulation is out of the scope of this paper, we just estimate R_0 using the exponential growth models employed in the SIR literature (Biggerstaff et al., 2014), and applied to COVID-19 by Agosto et al. (2020). More specifically, the exponential growth model of contagion assumes that the number of positive cases follow a Poisson distribution, with a growth parameter γ . This parameter can be estimated through the following regression: $\log N_t = k + \gamma * t$, where N_t is the cumulative number of positive cases up to t ; t is the time trend since the outbreak of the epidemic. Then the “instantaneous” reproduction rate $r_0 = \frac{f(1-\alpha)}{h}$ (Agosto et al., 2020) can be computed as the ratio between the fitted cases at t and the total number of fitted cases in the previous 8 days (assuming an incubation time equal to 7.5 days), i.e. $\hat{r}_0 = \frac{\hat{\gamma}_t}{\sum_{i=t-8}^t \hat{\gamma}_i}$. Finally, the estimated baseline R_0 can be computed as $\hat{R}_0 = \mathbb{E}(T) * \hat{r}_0 = 7.5 * \hat{r}_0$. To get an estimate of R_0 for each time period and province in our sample, we estimate a multilevel mixed-effects linear regression model of the cumulative number of cases in each province,¹⁹ i.e. $\log N_{it} = k_i + \gamma_i * t$. We then extract $\hat{\gamma}_i$ and multiply it by t to get the predicted province-specific level of positive cases at each day, $\hat{\gamma}_{it}$. We repeat this step for each of the 8 days before the time periods t in our sample, and get $\sum_{i=t-8}^{t-1} \hat{\gamma}_{it}$. With these numbers, following the formulae above, we finally compute the province-specific instantaneous reproduction rate as $\hat{r}_{0i} = \frac{\hat{\gamma}_{it}}{\sum_{i=t-8}^{t-1} \hat{\gamma}_{it}}$, and the baseline estimated reproduction rate as $\hat{R}_{0i} = 7.5 * \hat{r}_{0i}$. We therefore use the latter as a new measure of contagion, and re-estimate our pooled and fixed effect models using \hat{R}_{0i} as dependent variable. Results are reported in Table A5 in Appendix, and suggest that the positive relationship between pollution and contagion is confirmed also using this alternative dependent variable.

Our main estimates showed a robust association between quality of air and COVID-19 related outcomes. While we control for several characteristics of provinces, there might still be unobserved factors that are correlated both with pollution and the spread of the disease, thereby biasing our results. To mitigate this concern, we implement an instrumental variable (IV) approach relying on average wind speed in 2018 (the same year we consider for the pollution variables), in each province.²⁰ Our instrument is reasonably relevant since the wind level is negatively associated with pollution as highlighted by previous studies

(Keary et al., 1998; Chaloulakou et al., 2003; Aldrin and Haff, 2005; Akyüz and Çabuk, 2009; Pateraki et al., 2012). We assume that the exclusion restriction is satisfied since decreases and contagion during the COVID-19 epidemics in 2020 are hardly affected by wind speed in 2018, unless through pollution. It can be argued that the omission of wind speed in 2020 might invalidate the exclusion restriction, provided that historical wind speed is positively correlated with current wind speed, and that the current wind speed positively predicts the spread of contagion or mortality (Chen et al., 2020; Sahin et al., 2020). However, this does not seem to be a major concern in our case. Results from cross-section regressions of total deaths and total positive cases on the same factors as in Table 5 plus wind speed in 2018 show that the coefficient of the latter is negative and not statistically significant (available upon request). If wind speed in 2018 was serially correlated with current wind speed, and if the latter was also positively associated with the spread of the disease, we should have expected instead a positive and significant effect of wind speed in 2018 on COVID-19 outcomes in 2020. Yet, this is not the case in our data.

To implement the IV strategy, we estimate a pooled 2SLS regression instrumenting pollution with the natural logarithm of wind speed in 2018. In addition to the baseline controls, we stepwise include the three proxies for mobility – aggregated into one single variable (*mobility (pca)*) through a principal component analysis so to increase degrees of freedom – and economic activity, which in first-stage estimates turned out to be positively associated with pollution. First-stage estimates with all controls highlight a negative and significant effect of average wind speed in 2018 on PM levels ($\beta = -2.78$, $p = 0.019$ for PM10; $\beta = -2.56$, $p = 0.019$ for PM2.5); the instrument is not statistically significant for NO2 ($\beta = -1.47$, $p = 0.335$ for NO2), yet it becomes statistically significant ($\beta = -3.32$, $p = 0.038$) when we remove economic activity and mobility from the regressors.

Results from the second stage are reported in Table A6-A7 in the Appendix. The negative association between poor quality of air and new cases (Table A6) or new deaths (Table A7) is confirmed in most IV-estimates. Notice, however, that the inclusion of small-firms' economic activity (*Artisan*) weakens the effects of pollution; economic activity, moreover, turns insignificant in these estimates. These two results, jointly considered, suggest that the level of small-firms economic activity plays an indirect role in COVID-19 outcomes, that is it affects contagion and mortality mostly through pollution. Our preferred specifications are those in which neither mobility nor economic activity is controlled for. In facts, these model specifications outperform in terms of weak-instrument statistics. More specifically, the specifications excluding the two aforementioned regressors produce Kleibergen-Paap rk Wald F-statistics that are generally higher and closer to the Stock-Yogo weak ID test critical values allowing for a 10% maximal IV size. Moreover, in such specifications simple F-statistics from the first-stage regression reach the critical value of 10, while in models controlling also for mobility and economic activity first-stage F-statistics are well below that threshold.

We also replicate the IV approach exploiting the time dimension of the data. We estimate a fixed-effects panel 2SLS model adding the time trend, the squared time trend and the same interactions as in Table 7. We instrument the interaction between pollution and the time trend with the interaction between wind speed in 2018 (in logarithm) and the time trend. We also instrument the interaction between pollution and the *squared* time trend with the interaction between wind speed in 2018 (in logarithm) and the *squared* time trend. Results are reported in Table A7 and A8 for contagion and mortality, respectively. The interactions between pollution and the time trend variables are always statistically significant, and go in the same direction as those estimated in Table 7. Because province-specific fixed effects have been averaged out, we consider this model as the one that best controls for time-invariant

¹⁹ In an alternative specification of the contagion model, we also controlled for human mobility during the epidemic as computed by Pepe et al. (2020) (see footnote 17). Results do not change (available upon request).

²⁰ More specifically, we use as an instrument the natural logarithm of average wind speed in 2018 (meter/second) as registered by local environmental monitoring units. Data from the monitoring units have then been aggregated at the province level using municipality population weights so to give more importance to larger cities. Population weights are built considering the municipality where the monitoring units are located. Wind data have been obtained by ISPRA (“SCIA-ISPRA Ambiente” dataset), and complemented with data from the Italian Air Force in order to expand geographic coverage.

unobserved cofactors. Thus, the robustness of our results to the IV approach also in this model leads us to interpret the estimated statistical associations as causal.

7. Discussion

Our findings have several limitations and implications for future research. The statistical significance of our regressors does not necessarily imply causality and, based on the characteristics of our data, we do not have the possibility to test causality through a proper counterfactual trend or through RCTs. Indeed, it is impossible to build a properly randomized control group for a phenomenon that is already occurring at the time of the evaluation. In other words, we cannot create treatment and control groups with balanced baseline characteristics, “inoculate” the virus into the former group and compare the reactions among the two groups. However, the statistical significance of the three significant predictors (quality of air, economic activity and lockdown) withstands a barrage of robustness checks, including – most noticeably – instrumental variable estimates. Furthermore, the aforementioned predicted counterfactual analysis is, to the best of our knowledge, the closest approach to the first-best comparison between actual and counterfactual dynamics.

We also acknowledge a number of limitations in the quality of data. First, the COVID-19 test policy in Italy, especially at the onset of the pandemic, was different over time and across regions. Initially, tests were performed to suspected patients who present to hospital and/or people who have been in contact with positive cases; then, only patients with severe symptoms were tested. Then, tests were also performed to suspected people with no severe symptoms. In addition, some regions and provinces, adopted a policy to test only patients with severe symptoms in different periods²¹. Second, the available data on mortality record aggregate deaths and, therefore, we cannot disentangle COVID-19 deaths from deaths due to other diseases. More research is needed on the refinement of these dependent variables.

Finally, our estimates of the lockdown effects at municipality level might also be subject to bias. First, fixed-effects estimates, while netting out important unobserved time-invariant confounders, might not consider time-variant factors that could influence mortality over time, such as, for instance, the ability of local administrations to effectively respond to the dynamic of the virus, the decision of firms and individuals to comply (or not) with the restrictions, or the behavior of citizens regarding social interactions and sanitation measures (independently from lockdown). Responsive and efficient local administrations or the presence of highly prudent citizens might reduce the distance between the actual and the estimated counterfactual trend. While we run a series of robustness checks controlling for variables that could potentially address these concerns, we cannot be entirely sure that these factors capture all potential sources of unobserved (time-varying) heterogeneity across municipalities. Moreover, measurement error and non-perfect forecasting might also be an issue for our estimates; unfortunately, in spite of several requests, we did not get access to more precise data neither on contagion and recovery at the municipality level nor on mortality specifically due to COVID-19. Notwithstanding all these problems, our estimates, overall, seem to suggest that the lockdown decisions might have been effective in reducing mortality.

8. Conclusions

Our investigation originates from the observation of the uneven distribution of contagion across Italian provinces at the onset the

pandemic. The survey of the literature on drivers of COVID-19 and other respiratory diseases suggests that lockdown decisions and quality of air can play a role.

Our findings show that spread and severity of contagion is significantly associated with lockdown decisions, to factors affecting the quality of air and to the intensity of small business activity. These findings are robust to the use of different methodological approaches such as cross-section, pooled, fixed-effect OLS and instrumental variable regressions as well as to DiD estimates exploiting a simulated counterfactual trend, against which we benchmark the effect of lockdown and of its interaction with past levels of pollution.

The presence of micro (artisan) firms is positively correlated with contagion and mortality, suggesting, on the one hand, a certain degree of resistance by small business to lockdown policies, and, on the other, the presence of high economic activity, which conceals human interactions (and hence the spread of the disease). We also find evidence of an indirect effect of the presence of such firms on COVID-19 outcomes, i. e. through increased pollution.

Two important conclusions can be drawn from our findings. First, notwithstanding the aforementioned methodological caveats, lockdowns seem to be rather effective in limiting contagion and mortality during the first pandemic wave. Second, the quality of air is a strong predictor of contagion and mortality, suggesting that particulate “matters”: pre-existing levels of PM₁₀, PM_{2.5} and NO₂ are positively correlated with both the COVID-19 outcomes under investigation.

Several policy implications can be drawn if our estimates can be interpreted as causal. Some of the factors significantly correlated with COVID-19 outcomes are under human controls: lockdown policies, economic activity and, for most part, pollution. With reference to the latter, sources of particulate matter are for the most part (urban heating, transportation; energy; industry and agriculture) under our control, with only a small share depending on factors outside our control, such as atmospheric dusts (see footnote 8).

Hence it is in our power to reduce exposure of the global community to this risk factor. The most effective action concerns improved ecological efficiency of urban heating, and efforts to reduce the impact of mobility on pollution; sources of energy and production in industry and agriculture are also important.

Financial disclosure

The paper has not received any financial support.

Availability of data and code

Data and codes will be available upon request.

Credit author statement

Leonardo Becchetti, Pierluigi Conzo, Francesco Salustri: Conceptualization, Methodology, Formal analysis, Writing (Original Draft, Review & Editing), **Gianluigi Conzo:** Data curation, Investigation, Methodology, Formal analysis.

Declaration of competing interest

The authors declare that they have no known competing financial interests or personal relationships that could have appeared to influence the work reported in this paper.

We declare we have no conflicts of interest.

²¹ For instance, in the municipality of Vo’ all population was tested on 28 February 2020 (source: https://www.ansa.it/sito/notizie/cronaca/2020/02/28/zaia-d-a-test-vo-studio-epidemiologico_2c3d88f3-6a4a-4e00-b255-9e1e2feb2768.html).

APPENDIX A

Table A1

The effects of lockdown and pollution in reducing mortality (*DID approach*)

Dep. Var: <i>predicted mortality trends</i>	(1)	(2)	(3)	(4)	(5)	(6)	(7)	(8)
Lockdown	0.150*** (0.0220)	0.109*** (0.00866)	0.117*** (0.00807)	0.118*** (0.00903)				
Lockdown*Real trend	−0.130*** (0.0207)	−0.0918*** (0.00862)	−0.100*** (0.00796)	−0.101*** (0.00881)				
Lockdown*Pm2.5 ≥ median		0.0940*** (0.0264)						
Lockdown*Real trend* Pm2.5 ≥ median		−0.0890*** (0.0247)						
Lockdown*Pm10 ≥ median			0.0675** (0.0303)					
Lockdown*Real trend* Pm10 ≥ median			−0.0629** (0.0286)					
Lockdown*NO2 ≥ median				0.0677** (0.0272)				
Lockdown*Real trend* NO2 ≥ median				−0.0633** (0.0256)				
After 12/3					0.171*** (0.0279)	0.117*** (0.00950)	0.126*** (0.00888)	0.129*** (0.0106)
After 12/3*Real trend					−0.154*** (0.0268)	−0.102*** (0.00945)	−0.112*** (0.00881)	−0.114*** (0.0104)
After 12/3*Pm2.5 ≥ median						0.114*** (0.0304)		
After 12/3*Real trend* Pm2.5 ≥ median						−0.110*** (0.0290)		
After 12/3*Pm10 ≥ median							0.0875** (0.0343)	
After 12/3*Real trend* Pm10 ≥ median							−0.0840** (0.0329)	
After 12/3*NO2 ≥ median								0.0852** (0.0306)
After 12/3*Real trend* NO2 ≥ median								−0.0817** (0.0293)
Constant	0.0766*** (0.00895)	0.0734*** (0.00545)	0.0750*** (0.00784)	0.0751*** (0.00724)	0.0759*** (0.0101)	0.0748*** (0.00551)	0.0754*** (0.00798)	0.0754*** (0.00739)
Observations	174,536	169,380	173,870	173,242	174,536	169,380	173,870	173,242
R-squared	0.193	0.212	0.202	0.202	0.299	0.333	0.318	0.318
Number of municipalities	11,522	11,122	11,466	11,408	11,522	11,122	11,466	11,408

Dependent variable: previously estimated trend in mortality, i.e. $Mortality_{mt}$, which is equal to $\widehat{C_Mortality}_{mt}$ for the “cloned” observations to which we have assigned the predicted counterfactual trend, and to $\widehat{T_Mortality}_{mt}$ for original observations, to which we have assigned the (real) predicted mortality trend (see section 5); $Real_trend_m$ is the *treatment* indicator, which is equal to one for municipalities with the *real* mortality trend, and zero for their “clones” receiving the counterfactual trend. We use as post-treatment variable the dummy $Lockdown_{it}$, which is equal to one if the municipality m in province i in day t was under the total block, or the dummy $After_12/3_t$, which is equal to one for $t > March\ 12th, 2020$. The interaction $Lockdown_{it} * Real_trend_m$ or $After_12/3_t * Real_trend_m$ (i.e. the interaction between treatment and post-treatment indicator) is the DiD coefficient; standard errors are clustered at regional level; ***p < 0.01, **p < 0.05, *p < 0.1.

Table A2

Major factors explaining variation in mortality and contagion (*negative binomial model*)

Dep. Var.:	(1)	(2)	(3)	(4)	(5)	(6)
	<i>New_cases_pc</i>			<i>New_deaths_pc</i>		
Pm10	0.0670*** (0.0212)			0.0434*** (0.0118)		
Pm2.5		0.0756*** (0.0274)			0.0504*** (0.0185)	
No2			0.0396*** (0.0105)			0.0287*** (0.00733)
Observations	5086	4768	5033	4992	4680	4940

Negative binomial regression with time variable as offset. Standard errors are clustered at regional level.

***p < 0.01, **p < 0.05, *p < 0.1.

Table A3Major factors explaining variation in mortality and contagion (*weekly data*)

Dep. Var.:	(1)	(2)	(3)	(4)	(5)	(6)
	<i>New_cases_pc</i>			<i>New_deaths_pc</i>		
Pm10	0.0215** (0.0102)			0.00157** (0.000571)		
Pm2.5		0.0284** (0.0130)			0.00193** (0.000837)	
No2			0.0108** (0.00383)			0.000919*** (0.000263)
Week (<i>Ref</i> = 24-25 Feb)						
26 Feb – 3 Mar	0.0475* (0.0267)	0.0507* (0.0280)	0.0480* (0.0269)	−0.000625 (0.00108)	−0.000605 (0.00119)	−0.000582 (0.00108)
4 Mar – 10 Mar	0.135** (0.0642)	0.144** (0.0669)	0.136** (0.0647)	0.00704* (0.00395)	0.00776* (0.00412)	0.00691* (0.00399)
11–17 Mar	0.328*** (0.107)	0.347*** (0.110)	0.330*** (0.109)	0.0116 (0.00724)	0.0128 (0.00750)	0.0117 (0.00733)
18–24 Mar	0.604*** (0.146)	0.638*** (0.148)	0.607*** (0.148)	0.0197** (0.00896)	0.0213** (0.00926)	0.0193** (0.00907)
25–31 Mar	0.627*** (0.120)	0.657*** (0.120)	0.629*** (0.121)	0.0158** (0.00702)	0.0176** (0.00716)	0.0151** (0.00710)
1–7 Apr	0.554*** (0.0973)	0.580*** (0.0965)	0.543*** (0.0950)	−0.00236 (0.00382)	−0.00139 (0.00382)	−0.00214 (0.00386)
8–14 Apr	0.463*** (0.0622)	0.487*** (0.0628)	0.455*** (0.0595)	−0.00562* (0.00280)	−0.00441 (0.00302)	−0.00531* (0.00280)
Constant	−0.956*** (0.256)	−0.316 (0.326)	−0.488 (0.316)	−0.0399 (0.0237)	−0.00542 (0.0278)	−0.00823 (0.0276)
Controls	Yes	Yes	Yes	Yes	Yes	Yes
Observations	768	720	760	768	720	760
R-squared	0.490	0.492	0.474	0.336	0.328	0.316

Pooled OLS model. Controls are as in equation (1). Standard errors in parenthesis are clustered at regional level. ***p < 0.01, **p < 0.05, *p < 0.1.

Table A4Major factors explaining variation in mortality and contagion (*weekly data*)

Dep. Var.:	(1)	(2)	(3)	(4)	(5)	(6)
	<i>New_cases_pc</i>			<i>New_deaths_pc</i>		
Week (<i>Ref</i> = 24-25 Feb)						
(26 Feb – 3 Mar)*Pm10	0.0125* (0.00675)			0.000494** (0.000219)		
(4 Mar – 10 Mar)*Pm10	0.0243 (0.0146)			0.00122** (0.000569)		
(11–17 Mar)*Pm10	0.0313* (0.0173)			0.00229** (0.000959)		
(18–24 Mar)*Pm10	0.0388** (0.0182)			0.00262** (0.00111)		
(25–31 Mar)*Pm10	0.0238 (0.0141)			0.00168*** (0.000559)		
(1–7 Apr)*Pm10	0.0210** (0.00935)			0.00160*** (0.000417)		
(8–14 Apr)*Pm10	0.0201* (0.0115)			0.00114** (0.000400)		
Week (<i>Ref</i> = 24-25 Feb)						
(26 Feb – 3 Mar)*Pm2.5		0.0142** (0.00615)			0.000413 (0.000329)	
(4 Mar – 10 Mar)*Pm2.5		0.0303* (0.0157)			0.00170** (0.000698)	
(11–17 Mar)*Pm2.5		0.0417* (0.0214)			0.00320* (0.00157)	
(18–24 Mar)*Pm2.5		0.0520* (0.0251)			0.00357** (0.00145)	
(25–31 Mar)*Pm2.5		0.0353* (0.0196)			0.00237** (0.00101)	
(1–7 Apr)*Pm2.5		0.0267** (0.0121)			0.00153** (0.000645)	
(8–14 Apr)*Pm2.5		0.0254 (0.0164)			0.00168*** (0.000560)	
Week (<i>Ref</i> = 24-25 Feb)						
(26 Feb – 3 Mar)*No2			0.00462 (0.00277)			0.000362** (0.000140)
(4 Mar – 10 Mar)* No2			0.00837 (0.00541)			0.000769** (0.000324)
(11–17 Mar)* No2			0.0122*			0.00102**

(continued on next page)

Table A4 (continued)

Dep. Var.:	(1)	(2)	(3)	(4)	(5)	(6)
	<i>New_cases_pc</i>			<i>New_deaths_pc</i>		
(18–24 Mar)* No2			(0.00683) 0.0168**			(0.000402) 0.00125**
(25–31 Mar)* No2			(0.00693) 0.0122*			(0.000525) 0.00129***
(1–7 Apr)* No2			(0.00600) 0.0148***			(0.000311) 0.000880***
(8–14 Apr)* No2			(0.00439) 0.0156**			(0.000260) 0.000555**
			(0.00604) (1.158)			(0.000205) (0.0766)
Week (<i>Ref</i> = 24–25 Feb)						
26 Feb – 3 Mar	0.307 (0.331)	0.666 (0.496)	0.571 (0.473)	–0.00513 (0.0110)	–0.000187 (0.00980)	0.00387 (0.00976)
4 Mar – 10 Mar	0.333 (0.482)	1.032 (0.703)	0.847 (0.701)	–0.0196 (0.0251)	0.0218 (0.0386)	0.00618 (0.0352)
11–17 Mar	–0.416 (0.544)	0.488 (0.628)	0.234 (0.680)	–0.0504 (0.0302)	0.0117 (0.0293)	–0.00260 (0.0304)
18–24 Mar	–1.189* (0.650)	0.0764 (0.573)	–0.486 (0.577)	–0.0904* (0.0481)	–0.0254 (0.0464)	–0.0265 (0.0318)
25–31 Mar	–1.080* (0.561)	–0.186 (0.455)	–0.714 (0.470)	–0.116*** (0.0262)	–0.0608* (0.0293)	–0.0703** (0.0249)
1–7 Apr	–2.225*** (0.746)	–1.636* (0.833)	–1.640** (0.660)	–0.0997*** (0.0226)	–0.0592** (0.0217)	–0.0787*** (0.0219)
8–14 Apr	–1.764*** (0.495)	–1.154* (0.554)	–1.217*** (0.419)	–0.125*** (0.0270)	–0.0851*** (0.0256)	–0.111*** (0.0249)
Constant	0.811 (0.675)	0.955 (0.632)	0.902*** (0.160)	0.0714* (0.0376)	0.0662 (0.0453)	0.0396*** (0.00773)
Week dummies*Controls	Yes	Yes	Yes	Yes	Yes	Yes
Observations	768	720	760	768	720	760
R-squared	0.650	0.656	0.641	0.398	0.403	0.381
Number of provinces	96	90	95	96	90	95

Panel FE model. Controls are as in equation (1). Standard errors in parenthesis are clustered at regional level.

***p < 0.01, **p < 0.05, *p < 0.1.

Table A5

Pollution and province-specific estimated reproduction rate of COVID-19

Dep. Var.: \widehat{R}_{0i}	(1)	(2)	(3)	(4)	(5)	(6)
Day	–0.00823*** (2.39e-05)	–0.00823*** (2.62e-05)	–0.00823*** (2.43e-05)	–0.00839*** (0.000102)	–0.00843*** (9.75e-05)	–0.00827*** (7.64e-05)
Day ²	5.39e-05*** (2.57e-07)	5.39e-05*** (2.81e-07)	5.39e-05*** (2.59e-07)	5.55e-05*** (7.58e-07)	5.57e-05*** (6.29e-07)	5.44e-05*** (5.30e-07)
Pm10	5.05e-05** (2.17e-05)					
Pm2.5		4.63e-05* (2.63e-05)				
No2			4.11e-05** (1.77e-05)			
Day*PM10				4.84e-06* (2.47e-06)		
Day ² *PM10				–5.02e-08* (2.58e-08)		
Day*PM2.5					8.46e-06** (3.01e-06)	
Day ² *PM2.5					–9.20e-08*** (3.04e-08)	
Day*NO2						1.10e-06 (2.07e-06)
Day ² *NO2						–8.92e-09 (2.22e-08)
Constant	1.311*** (0.00151)	1.313*** (0.00163)	1.312*** (0.00158)	1.311*** (0.000608)	1.311*** (0.000623)	1.311*** (0.000666)
Controls	Yes	Yes	Yes	Yes	Yes	Yes
Observations	6037	5659	5974	6037	5659	5974
R-squared	0.982	0.982	0.982	0.982	0.982	0.982
Number of provinces				96	90	95

Pooled OLS regressions in columns 1–3; Panel FE regressions in columns 4–6. Standard errors are clustered at regional level. Controls are as in Eq. 2.

***p < 0.01, **p < 0.05, *p < 0.1.

Table A6Pollution and contagion (*Instrumental Variable OLS Pooled Regressions – second stage*)

Dep. Var.: New cases per 1,000 inhabitants	(1)	(2)	(3)	(4)	(5)	(6)	(7)	(8)	(9)
PM10	0.0154*** (0.00406)	0.0147*** (0.00412)	0.0105** (0.00481)						
PM2.5				0.0135*** (0.00366)	0.0136*** (0.00397)	0.0113* (0.00626)			
NO2							0.0176** (0.00756)	0.0194* (0.0104)	0.0198 (0.0243)
Day	0.0106*** (0.00228)	0.0106*** (0.00228)	0.0107*** (0.00229)	0.0112*** (0.00236)	0.0112*** (0.00236)	0.0113*** (0.00237)	0.0103*** (0.00228)	0.0102*** (0.00229)	0.0103*** (0.00229)
Day ²	−9.09e-05*** (2.16e-05)	−9.10e-05*** (2.16e-05)	−9.17e-05*** (2.17e-05)	−9.66e-05*** (2.25e-05)	−9.66e-05*** (2.25e-05)	−9.73e-05*** (2.26e-05)	−8.74e-05*** (2.16e-05)	−8.69e-05*** (2.16e-05)	−8.75e-05*** (2.17e-05)
Mobility (pca)		0.00624 (0.0111)	0.00282 (0.00901)		−0.00290 (0.00950)	−0.00396 (0.00799)		−0.0160 (0.0239)	−0.0151 (0.0284)
Artisan			0.330* (0.179)			0.216 (0.280)			−0.0369 (0.889)
Urban green	−0.00230 (0.00181)	−0.00268 (0.00170)	−0.00199 (0.00150)	−0.00438** (0.00156)	−0.00424*** (0.00138)	−0.00384*** (0.00116)	−0.00278 (0.00398)	−0.00184 (0.00485)	−0.00180 (0.00477)
High temperature	−0.00839 (0.0206)	−0.00675 (0.0181)	−0.00316 (0.0149)	0.0180 (0.0150)	0.0176 (0.0147)	0.0164 (0.0146)	−0.0673** (0.0316)	−0.0776* (0.0414)	−0.0782 (0.0900)
Density	−2.74e-05 (1.91e-05)	−3.18e-05 (2.10e-05)	−1.78e-05 (2.21e-05)	−1.55e-05 (1.64e-05)	−1.32e-05 (1.48e-05)	−7.13e-06 (1.83e-05)	−0.000138 (8.51e-05)	−0.000138 (8.85e-05)	−0.000141 (0.000199)
Over65	0.000451 (0.000510)	0.000344 (0.000542)	−6.99e-05 (0.000467)	−0.000260 (0.000389)	−0.000228 (0.000410)	−0.000378 (0.000372)	−0.000146 (0.000660)	6.64e-05 (0.000695)	7.94e-05 (0.000967)
Income	0.372** (0.144)	0.366** (0.144)	0.273** (0.123)	0.352*** (0.116)	0.355*** (0.119)	0.299* (0.143)	0.382* (0.213)	0.398 (0.250)	0.410 (0.465)
Health (pca)	−0.00177 (0.00353)	−0.00276 (0.00330)	−0.00144 (0.00256)	−0.00132 (0.00327)	−0.000761 (0.00292)	−0.000139 (0.00219)	−0.00330 (0.00409)	−0.000920 (0.00504)	−0.000973 (0.00522)
Constant	−0.736*** (0.176)	−0.693*** (0.195)	−0.577*** (0.179)	−0.413*** (0.0854)	−0.424*** (0.105)	−0.409*** (0.104)	−0.540*** (0.152)	−0.629** (0.249)	−0.633 (0.444)
Observations	4874	4874	4821	4556	4556	4503	4927	4927	4874
Centered R-squared	−0.087	−0.048	0.167	0.142	0.138	0.201	−0.648	−0.845	−0.892
Kleibergen-Paap rk Wald F statistic	11.25	9.215	6.335	11.34	9.617	6.886	6.284	3.853	0.988

Results from second-stage IV pooled regression model. Instrument: *wind speed in 2018*; Instrumented variables: PM10 (col. 1–3), PM2.5 (col. 4–6), NO2 (col. 7–9). Standard errors are clustered at regional level; ***p < 0.01, **p < 0.05, *p < 0.1.

Table A7Pollution and mortality (*Instrumental Variable OLS Pooled Regressions – second stage*)

Dep. Var.: New deaths per 1,000 inhabitants	(1)	(2)	(3)	(4)	(5)	(6)	(7)	(8)	(9)
PM10	0.00518** (0.00223)	0.00536** (0.00228)	0.00331 (0.00217)						
PM2.5				0.00473** (0.00206)	0.00505** (0.00218)	0.00376 (0.00269)			
NO2							0.00592* (0.00308)	0.00702 (0.00410)	0.00625 (0.00845)
Day	0.00371** (0.00136)	0.00371** (0.00136)	0.00374** (0.00137)	0.00388** (0.00144)	0.00388** (0.00144)	0.00391** (0.00145)	0.00364** (0.00134)	0.00363** (0.00134)	0.00366** (0.00134)
Day ²	−3.79e-05*** (1.31e-05)	−3.79e-05*** (1.31e-05)	−3.82e-05*** (1.32e-05)	−3.95e-05*** (1.40e-05)	−3.95e-05*** (1.39e-05)	−3.98e-05*** (1.40e-05)	−3.71e-05*** (1.30e-05)	−3.69e-05*** (1.30e-05)	−3.73e-05*** (1.30e-05)
Mobility (pca)		−0.00175 (0.00365)	−0.00355 (0.00256)		−0.00502 (0.00345)	−0.00568** (0.00263)		−0.00980 (0.00882)	−0.00923 (0.00956)
Artisan			0.159** (0.0658)			0.120 (0.0952)			0.0432 (0.301)
Urban green	−0.00116* (0.000583)	−0.00105* (0.000585)	−0.000734 (0.000544)	−0.00187** (0.000710)	−0.00164** (0.000702)	−0.00142** (0.000641)	−0.00132 (0.00134)	−0.000742 (0.00171)	−0.000672 (0.00157)
High temperature	0.00109 (0.00617)	0.000613 (0.00619)	0.00190 (0.00444)	0.0105 (0.00634)	0.00979 (0.00601)	0.00887 (0.00583)	−0.0235 (0.0141)	−0.0308 (0.0179)	−0.0268 (0.0368)
Density	−1.42e-05* (7.84e-06)	−1.30e-05 (7.83e-06)	−6.33e-06 (7.54e-06)	−1.10e-05 (7.86e-06)	−6.88e-06 (5.55e-06)	−3.57e-06 (6.40e-06)	−5.13e-05 (3.38e-05)	−5.12e-05 (3.41e-05)	−4.50e-05 (6.82e-05)
Over65	0.000243 (0.000163)	0.000273 (0.000194)	7.68e-05 (0.000159)	2.36e-05 (0.000179)	7.90e-05 (0.000173)	−2.84e-06 (0.000146)	4.24e-05 (0.000221)	0.000173 (0.000250)	0.000126 (0.000313)
Income	0.102* (0.0551)	0.104* (0.0565)	0.0582 (0.0470)	0.0820 (0.0511)	0.0878 (0.0518)	0.0561 (0.0586)	0.104 (0.0728)	0.113 (0.0900)	0.100 (0.157)

(continued on next page)

Table A7 (continued)

Dep. Var.: <i>New deaths per 1,000 inhabitants</i>	(1)	(2)	(3)	(4)	(5)	(6)	(7)	(8)	(9)
Health (pca)	−0.00104 (0.00118)	−0.000763 (0.00106)	−0.000133 (0.000680)	−0.00125 (0.00125)	−0.000295 (0.00100)	4.74e-05 (0.000702)	−0.00155 (0.00124)	−9.08e-05 (0.00160)	1.81e-05 (0.00151)
Constant	−0.235** (0.0868)	−0.246** (0.0953)	−0.192** (0.0828)	−0.131** (0.0456)	−0.150** (0.0524)	−0.142** (0.0504)	−0.169** (0.0622)	−0.224** (0.104)	−0.210 (0.162)
Observations	4784	4784	4732	4472	4472	4420	4836	4836	4784
Centered R-squared	0.028	0.005	0.269	0.183	0.183	0.273	−0.546	−0.858	−0.587
Kleibergen-Paap rk Wald F statistic	11.22	9.205	6.336	11.30	9.584	6.889	6.361	3.904	1.003

Results from second-stage IV pooled regression model. Instrument: *wind speed in 2018*; Instrumented variables: PM10 (col. 1–3), PM2.5 (col. 4–6), NO2 (col. 7–9). Standard errors are clustered at regional level; ***p < 0.01, **p < 0.05, *p < 0.1.

Table A8

Pollution and contagion (*Instrumental Variable OLS Pooled Regressions – second stage*). Results from second-stage IV fixed-effects panel regression model. Instruments: *wind speed in 2018*day*, *wind speed in 2018*day²*; Instrumented variables: PM10*day and PM10*day² (col. 1–3), PM2.5*day and PM2.5*day² (col. 4–6), NO2*day and NO2*day² (col. 7–9). Standard errors are clustered at regional level; ***p < 0.01, **p < 0.05, *p < 0.1.

Dep. Var.: <i>New cases per 1,000 inhabitants</i>	(1)	(2)	(3)	(4)	(5)	(6)	(7)	(8)	(9)
Day*PM10	0.00247*** (0.000688)	0.00230*** (0.000645)	0.00224*** (0.000643)						
Day ² *PM10	−2.23e-05*** (6.77e-06)	−2.15e-05*** (6.72e-06)	−2.15e-05*** (6.69e-06)						
Day*PM2.5				0.00195*** (0.000563)	0.00183*** (0.000514)	0.00178*** (0.000514)			
Day ² *PM2.5				−1.77e-05*** (5.88e-06)	−1.71e-05*** (5.54e-06)	−1.71e-05*** (5.54e-06)			
Day*NO2							0.00224*** (0.000784)	0.00230*** (0.000860)	0.00224** (0.000877)
Day ² *NO2							−2.01e-05*** (7.43e-06)	−2.11e-05*** (7.96e-06)	−2.11e-05*** (7.92e-06)
Day	−0.0496*** (0.0164)	−0.0508*** (0.0151)	−0.0491*** (0.0150)	−0.0193** (0.00800)	−0.0214*** (0.00783)	−0.0211*** (0.00777)	−0.0347** (0.0156)	−0.0407** (0.0173)	−0.0396** (0.0178)
Day ²	0.000451*** (0.000159)	0.000434*** (0.000158)	0.000434*** (0.000157)	0.000180** (8.32e-05)	0.000169** (7.68e-05)	0.000169** (7.69e-05)	0.000316** (0.000148)	0.000337** (0.000161)	0.000337** (0.000161)
Day*mobility (pca)		0.000231 (0.000224)	0.000175 (0.000204)		0.000172 (0.000265)	0.000148 (0.000252)		7.09e-05 (0.000369)	9.63e-05 (0.000374)
Day*Artisan			0.00479 (0.00298)			0.00444 (0.00421)			0.00322 (0.00644)
Day*Health (pca)		−5.12e-05 (4.00e-05)	−3.24e-05 (3.34e-05)		−3.13e-05 (3.90e-05)	−1.86e-05 (3.18e-05)		−3.85e-05 (5.14e-05)	−3.06e-05 (4.17e-05)
Day*Income		0.00219 (0.00347)	0.000813 (0.00337)		0.00200 (0.00354)	0.000820 (0.00376)		0.00260 (0.00384)	0.00152 (0.00499)
Day*Over65		2.15e-05* (1.15e-05)	1.57e-05 (1.28e-05)		1.70e-05 (1.13e-05)	1.40e-05 (1.23e-05)		1.97e-05** (8.86e-06)	1.65e-05 (1.30e-05)
Day*Density		−4.70e-08 (3.62e-07)	1.51e-07 (3.55e-07)		7.56e-08 (2.75e-07)	1.98e-07 (2.87e-07)		−8.28e-07 (1.20e-06)	−3.94e-07 (1.73e-06)
Day*Urban green		1.67e-07 (4.44e-05)	9.51e-06 (4.54e-05)		1.12e-06 (5.75e-05)	9.03e-06 (6.37e-05)		6.47e-06 (5.79e-05)	1.04e-05 (5.26e-05)
High temperature		−0.000724 (0.00564)	−0.000778 (0.00588)		−0.00457 (0.00410)	−0.00555 (0.00419)		0.00202 (0.00720)	0.00172 (0.00761)
Constant	−0.225*** (0.0426)	−0.227*** (0.0420)	−0.229*** (0.0410)	−0.237*** (0.0366)	−0.238*** (0.0385)	−0.240*** (0.0380)	−0.221*** (0.0537)	−0.225*** (0.0515)	−0.227*** (0.0509)
Observations	5300	4874	4821	4929	4556	4503	5406	4927	4874
Number of provinces	100	92	91	93	86	85	102	93	92
Overall R ²	0.0839	0.0999	0.106	0.128	0.139	0.145	0.0609	0.0607	0.0626

Results from second-stage IV fixed-effects panel regression model. Instruments: *wind speed in 2018*day*, *wind speed in 2018*day²*; Instrumented variables: PM10*day and PM10*day² (col. 1–3), PM2.5*day and PM2.5*day² (col. 4–6), NO2*day and NO2*day² (col. 7–9). Standard errors are clustered at regional level; *** p<0.01, ** p<0.05, * p<0.1.

Table A9
Pollution and mortality (Instrumental Variable OLS Pooled Regressions – second stage)

Dep. Var.: New deaths per 1,000 inhabitants	(1)	(2)	(3)	(4)	(5)	(6)	(7)	(8)	(9)
Day*PM10	0.00137*** (0.000510)	0.00130** (0.000540)	0.00126** (0.000538)						
Day ² *PM10	−1.32e-05*** (5.12e-06)	−1.27e-05** (5.44e-06)	−1.26e-05** (5.46e-06)						
Day*PM2.5				0.00115** (0.000484)	0.00110** (0.000503)	0.00107** (0.000499)			
Day ² *PM2.5				−1.12e-05** (4.88e-06)	−1.07e-05** (5.07e-06)	−1.08e-05** (5.08e-06)			
Day*NO2							0.00121** (0.000488)	0.00128** (0.000568)	0.00124** (0.000572)
Day ² *NO2							−1.17e-05** (4.89e-06)	−1.23e-05** (5.59e-06)	−1.22e-05** (5.60e-06)
Day	−0.0296** (0.0119)	−0.0289** (0.0126)	−0.0280** (0.0126)	−0.0141** (0.00693)	−0.0138* (0.00714)	−0.0136* (0.00714)	−0.0207** (0.00981)	−0.0229** (0.0115)	−0.0223* (0.0115)
Day ²	0.000284** (0.000119)	0.000270** (0.000126)	0.000270** (0.000127)	0.000135* (7.01e-05)	0.000128* (7.17e-05)	0.000128* (7.20e-05)	0.000197** (9.83e-05)	0.000211* (0.000112)	0.000211* (0.000113)
Day*mobility (pca)		5.40e-05 (4.45e-05)	2.08e-05 (2.58e-05)		2.53e-05 (4.45e-05)	9.20e-06 (3.30e-05)		−1.79e-05 (7.60e-05)	−4.75e-06 (5.99e-05)
Day*Artisan			0.00266*** (0.000676)			0.00282*** (0.00102)			0.00205 (0.00185)
Day*Health (pca)		−1.80e-05 (1.41e-05)	−7.66e-06 (1.03e-05)		−5.24e-06 (1.13e-05)	2.77e-06 (9.24e-06)		−1.31e-05 (2.01e-05)	−8.08e-06 (1.44e-05)
Day*Income		0.000949 (0.00102)	0.000177 (0.000918)		0.000986 (0.00110)	0.000233 (0.00106)		0.00121 (0.00108)	0.000525 (0.00123)
Day*Over65		4.21e-06** (2.12e-06)	1.03e-06 (2.06e-06)		2.13e-06 (2.37e-06)	2.54e-07 (2.15e-06)		3.20e-06 (2.54e-06)	1.19e-06 (2.28e-06)
Day*Density		−7.83e-08 (6.52e-08)	3.00e-08 (7.16e-08)		−1.90e-08 (5.37e-08)	5.92e-08 (6.25e-08)		−4.29e-07 (3.04e-07)	−1.58e-07 (4.14e-07)
Day*Urban green		0.00116 (0.00109)	0.000843 (0.00101)		0.00103 (0.00145)	0.000125 (0.00174)		0.00775 (0.00558)	0.00782 (0.00614)
High temperature		−2.37e-05** (1.13e-05)	−1.87e-05 (1.28e-05)		−2.23e-05 (1.45e-05)	−1.74e-05 (1.89e-05)		−2.06e-05 (1.98e-05)	−1.84e-05 (1.60e-05)
Constant	−0.0447* (0.0234)	−0.0463* (0.0255)	−0.0469* (0.0249)	−0.0478** (0.0216)	−0.0493** (0.0240)	−0.0500** (0.0236)	−0.0437* (0.0247)	−0.0460* (0.0253)	−0.0467* (0.0250)
Observations	5200	4784	4732	4836	4472	4420	5304	4836	4784
Number of provinces	100	92	91	93	86	85	102	93	92
Overall R ²	0.113	0.132	0.138	0.154	0.167	0.174	0.0599	0.0663	0.0676

Results from second-stage IV fixed-effects panel regression model. Instruments: *wind speed in 2018*day*, *wind speed in 2018*day²*; Instrumented variables: *PM10*day* and *PM10*day²* (col. 1–3), *PM2.5*day* and *PM2.5*day²* (col. 4–6), *NO2*day* and *NO2*day²* (col. 7–9). Standard errors are clustered at regional level; ***p < 0.01, **p < 0.05, *p < 0.1.

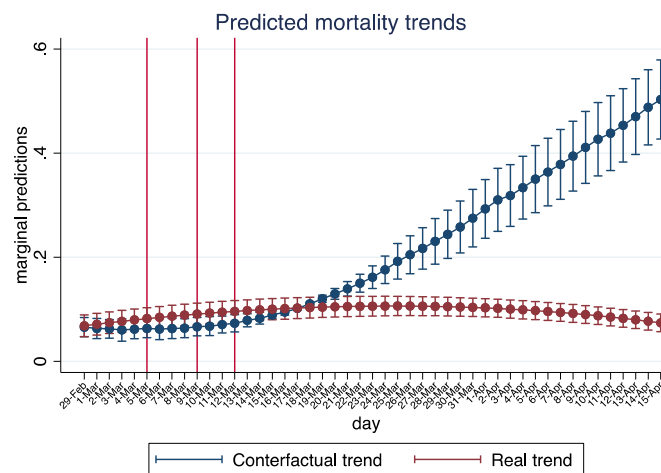


Fig. A1. COVID-19 mortality: real and counterfactual trend.

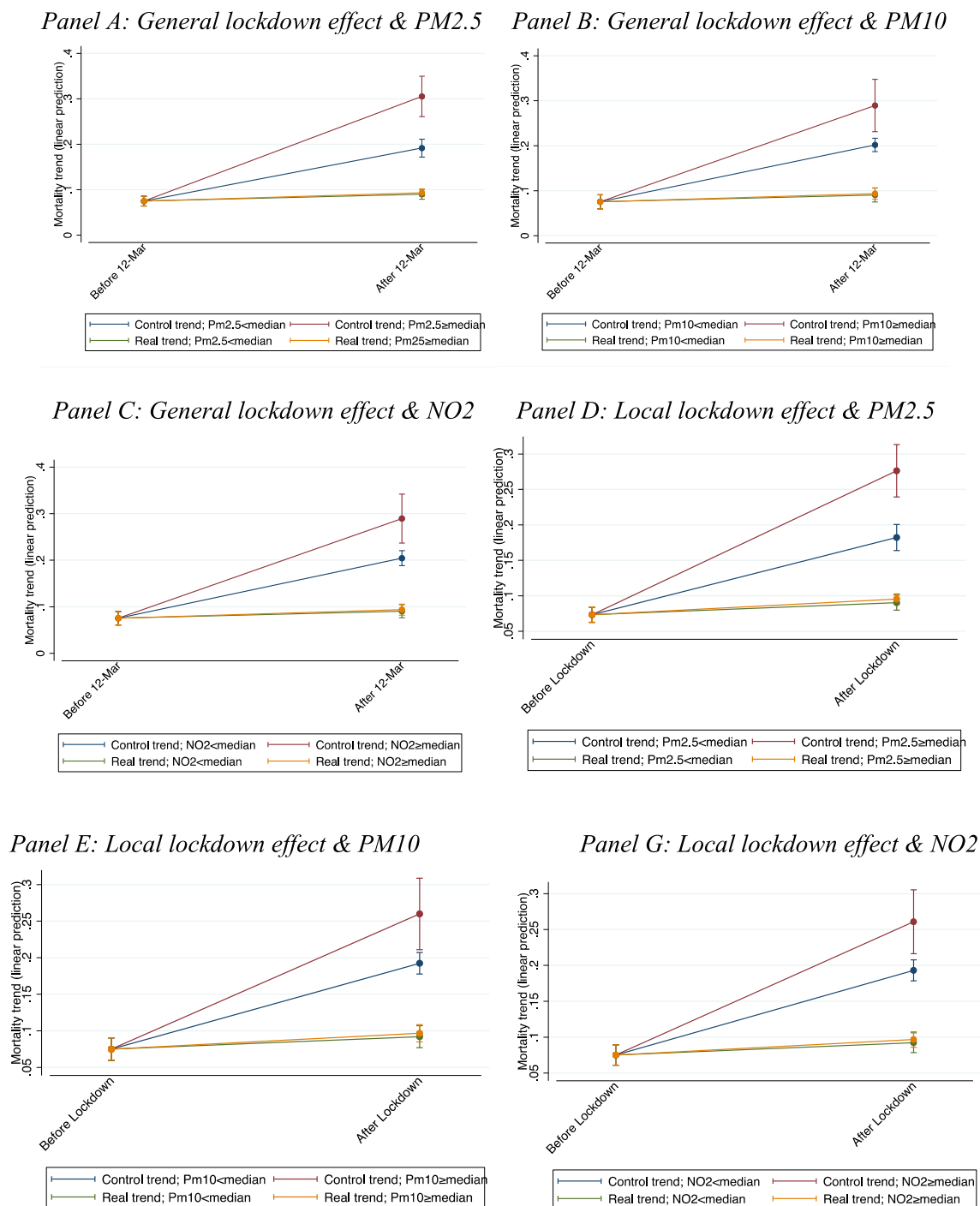


Fig. A2. COVID-19 mortality: mortality trends by lockdown and pollution.

APPENDIX B

Analysis of outliers

Descriptive analysis

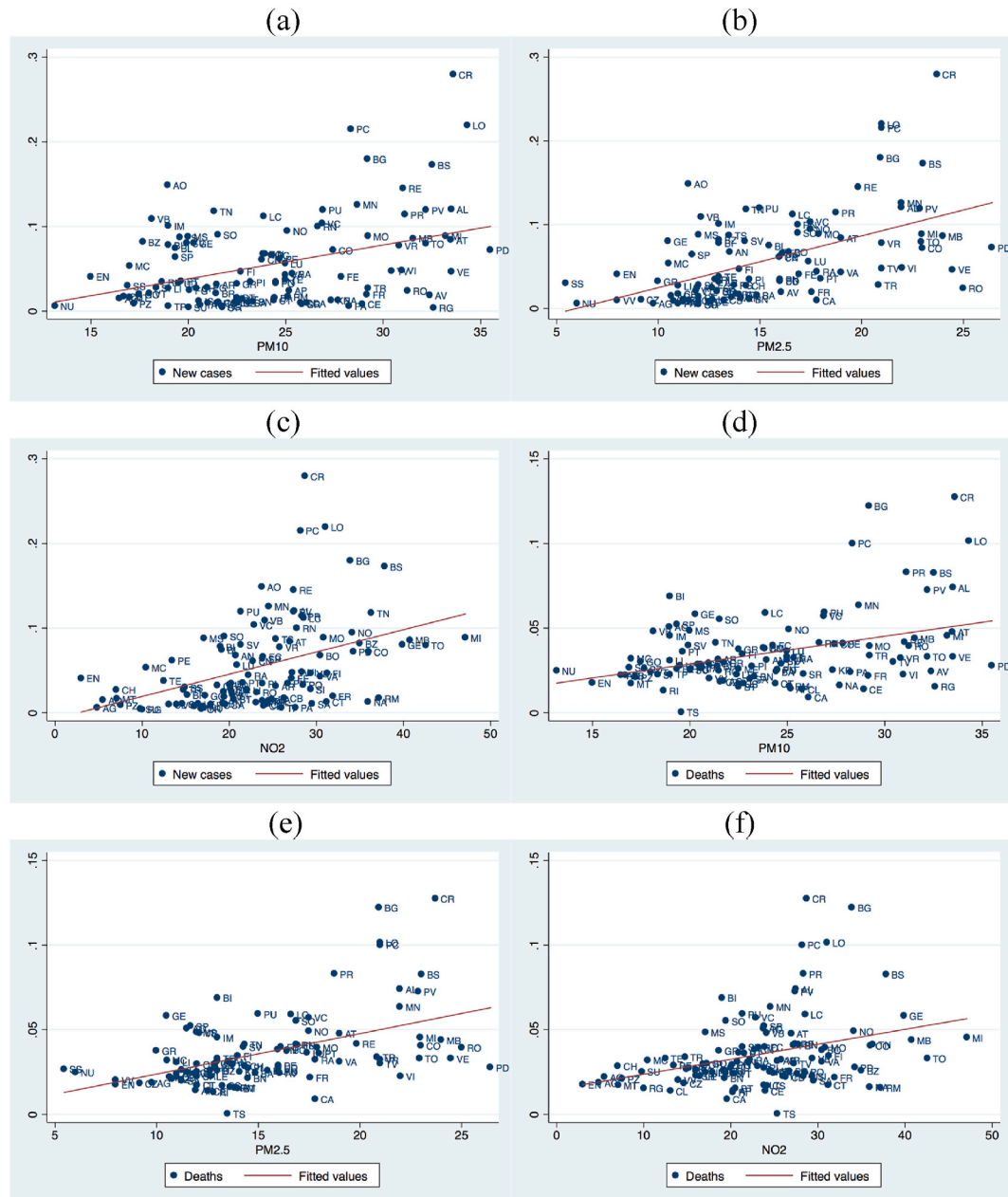


Fig. B1. Pollutants, contagions, and mortality in Italian provinces (average during the period 24 February – April 15, 2020, observed and linear fitted values).

Studentised residuals

Table B1 shows studentised residuals greater than 2. Residuals are obtained from pooled OLS model as in equation (1). The provinces with the highest residuals are Cremona, Piacenza, and Lodi.

Table B1
Extreme studentised residuals.

PM10		PM25		NO2	
r	Province	r	Province	r	Province
2.34	LO	2.53	LO	2.47	LO
3.35	PC	2.98	PC	3.43	PC
5.2	CR	4.96	CR	5.57	CR

Figure B2 show the leverages (obtained from pooled OLS model as in equation (1)) and the studentised residuals for each pollutant. Those with respect to PM10 and PM2.5 are very similar and show that the observations that may be problematic for leverages (i.e., SA, NA, TS, PN, MI) are different from those detected with studentised residuals.

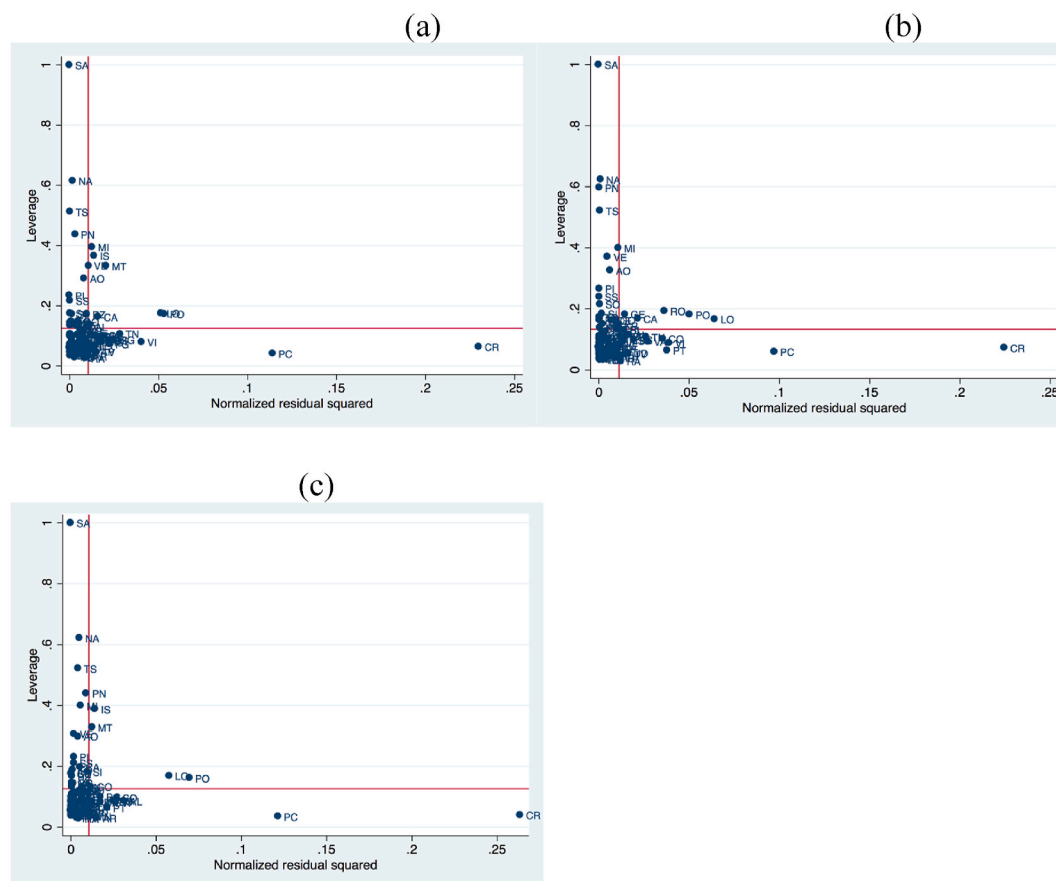


Fig. B2. Leverages and studentised residuals.

Figure B3 displays for each province the dfbeta for PM10, PM2.5, and NO2, respectively. The plot confirms that Cremona, Lodi, and Piacenza are the most “influential” observations. Depending on the pollutant, Prato, Trieste, Isernia, Matera, Ragusa, and Rovigo may also be highly influential.

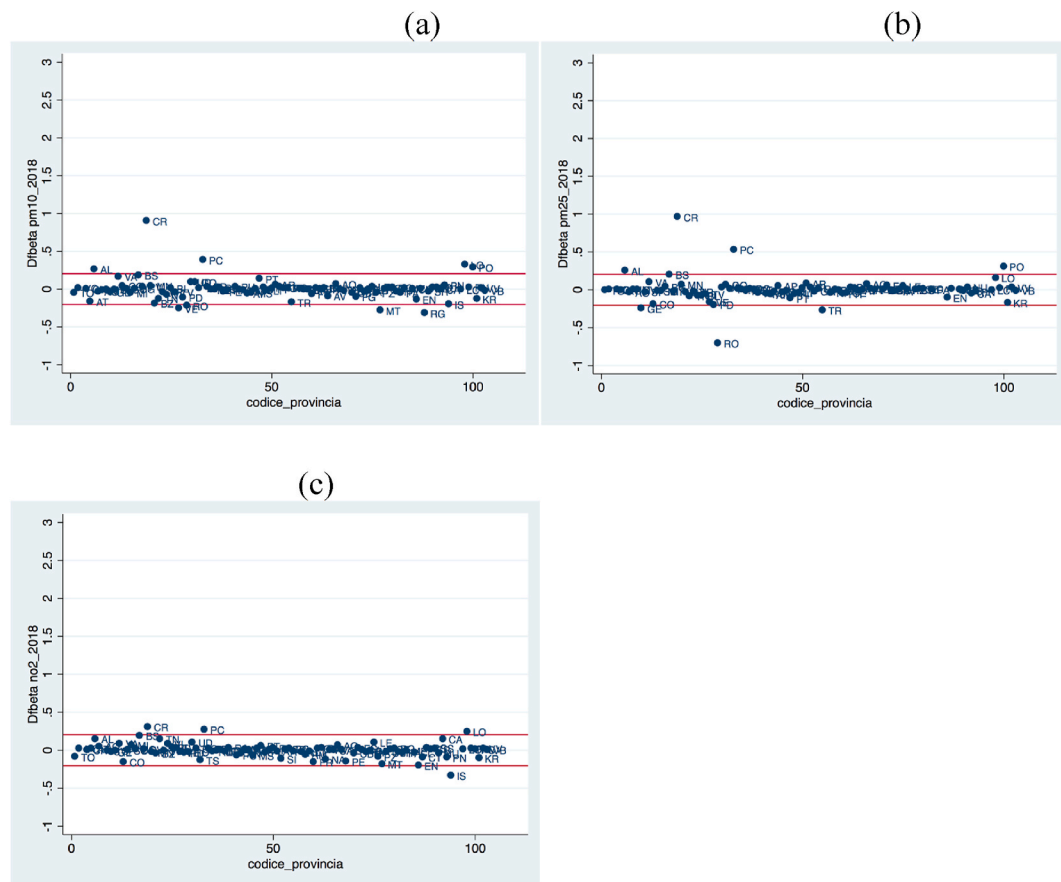


Fig. B3. DFBETA.

Table B2
Pollution, contagion, and mortality (excluding influential observations)

Dep. Var.	Pm10	Pm2.5	No2	Constant	Obs.	R ²
<i>Excluded provinces: Cremona, Lodi, Piacenza.</i>						
New_cases_pc	0.00207** (0.000947)			−0.424*** (0.0616)	4927	0.268
New_cases_pc		0.00253* (0.00128)		−0.378*** (0.0599)	4609	0.262
New_cases_pc			0.00124*** (0.000415)	−0.379*** (0.0532)	4874	0.288
New_deaths_pc	0.00106*** (0.000359)			−0.115*** (0.0251)	4836	0.286
New_deaths_pc		0.00128** (0.000607)		−0.0971*** (0.0246)	4524	0.275
New_deaths_pc			0.000645*** (0.000189)	−0.0952*** (0.0189)	4784	0.277
<i>Excluded provinces: Cremona, Lodi, Piacenza, Ragusa, Isernia, Rovigo, Trento, Matera.</i>						
New_cases_pc	0.00302*** (0.000900)			−0.437*** (0.0616)	4662	0.274
New_cases_pc		0.00342** (0.00122)		−0.383*** (0.0614)	4503	0.265
New_cases_pc			0.00152*** (0.000516)	−0.371*** (0.0557)	4609	0.290
New_deaths_pc	0.00127*** (0.000375)			−0.123*** (0.0269)	4576	0.295
New_deaths_pc		0.00144** (0.000662)		−0.0977*** (0.0251)	4420	0.277
New_deaths_pc			0.000685*** (0.000210)	−0.0974*** (0.0208)	4524	0.279

Standard errors in parenthesis are clustered at regional level.

References

- Akyüz, M., Çabuk, H., 2009. Meteorological variations of PM_{2.5}/PM₁₀ concentrations and particle-associated polycyclic aromatic hydrocarbons in the atmospheric environment of Zonguldak, Turkey. *J. Hazard Mater.* 170, 13–21. <https://doi.org/10.1016/j.jhazmat.2009.05.029>.
- Agosto, A., Campmas, A., Giudici, P., Renda, A., 2020. Monitoring Covid-19 contagion growth in Europe. In: CEPS Working Document No 2020/03. March 2020. <http://aei.pitt.edu/id/eprint/102672>.
- Aldrin, M., Haff, I.H., 2005. Generalised additive modelling of air pollution, traffic volume and meteorology. *Atmos. Environ.* 39, 2145–2155. <https://doi.org/10.1016/j.atmosenv.2004.12.020>.
- Bajardi, P., Poletto, C., Ramasco, J.J., Tizzoni, M., Colizza, V., Vespignani, A., 2011. Human mobility networks, travel restrictions, and the global spread of 2009 H1N1 pandemic. *PLoS One* 6 (1). <https://doi.org/10.1371/journal.pone.0016591>.
- Barreca, A.I., Shimshack, J.P., 2012. Absolute humidity, temperature, and influenza mortality: 30 years of county-level evidence from the United States. *Am. J. Epidemiol.* 176 (Suppl. 7), S114–S122. <https://doi.org/10.1093/aje/kws259>.
- Bannister-Tyrrell, M., Meyer, A., Faverjon, C., Cameron, A., 2020. Preliminary Evidence that Higher Temperatures Are Associated with Lower Incidence of COVID-19, for Cases Reported Globally up to 29th February 2020. medRxiv. <https://doi.org/10.1101/2020.03.18.20036731>.
- Biggerstaff, M., Cauchemez, S., Reed, C., Gambhir, M., Finelli, L., 2014. Estimates of the reproduction number for seasonal, pandemic, and zoonotic influenza: a systematic review of the literature. *BMC Infect. Dis.* 14 (1), 480. <https://doi.org/10.1186/1471-2334-14-480>.
- Bukhari, Qasim, Jameel, Yusuf, 2020. Will coronavirus pandemic diminish by summer? Available at: SSRN 3556998. <https://doi.org/10.2139/ssrn.3556998>.
- Chaloulakou, A., Kassomenos, P., Spyrellis, N., Demokritou, P., Koutarakis, P., 2003. Measurements of PM₁₀ and PM_{2.5} particle concentrations in Athens, Greece. *Atmos. Environ.* 37, 649–660. [https://doi.org/10.1016/S1352-2310\(02\)00898-1](https://doi.org/10.1016/S1352-2310(02)00898-1).
- Charu, V., Zeger, S., Gog, J., Bjørnstad, O.N., Kissler, S., Simonsen, L., Grenfell, B.T., Viboud, C., 2017. Human mobility and the spatial transmission of influenza in the United States. *PLoS Comput. Biol.* 13 (2), e1005382. <https://doi.org/10.1371/journal.pcbi.1005382>.
- Chen, B., Liang, H., Yuan, X., Hu, Y., Xu, M., Zhao, Y., et al., 2020. Roles of meteorological conditions in COVID-19 transmission on a worldwide scale. medRxiv. <https://doi.org/10.1101/2020.03.16.20037168>.
- Cereda, D., Tirani, M., Rovida, F., Demicheli, V., Ajelli, M., Poletti, P., Merler, S., 2020. The Early Phase of the COVID-19 Outbreak in Lombardy, Italy. <https://arxiv.org/abs/2003.09320>.
- Conticini, E., Frediani, B., Caro, D., 2020. Can atmospheric pollution be considered a co-factor in extremely high level of SARS-CoV-2 lethality in Northern Italy? *Environ. Pollut.* 114465. <https://doi.org/10.1016/j.envpol.2020.114465>.
- European Court of Auditors, 2018. Air pollution: EU citizens' health still not sufficiently protected, warn Auditors. Available at: https://www.eca.europa.eu/Lists/ECADocuments/INSR18_23/INSR_AIR_QUALITY_EN.pdf.
- Fang, H., Wang, L., Yang, Y., 2020. Human Mobility Restrictions and the Spread of the Novel Coronavirus (2019-ncov) in China (No. W26906). National Bureau of Economic Research. <https://doi.org/10.3386/w26906>.
- Gu, C., Jiang, W., Zhao, T., Zheng, B., 2020. Mathematical Recommendations to Fight against COVID-19. <https://doi.org/10.2139/ssrn.3551006>.
- ISPRA, 2018. XIII Rapporto Qualità Dell'ambiente Urbano - Edizione 2017. <https://www.isprambiente.gov.it/it/pubblicazioni/stato-dellambiente/xiii-rapporto-qualita-a-dell2019ambiente-urbano-edizione-2017>.
- Keary, J., Jennings, S.G., O'Connor, T.C., McManus, B., Lee, M., 1998. PM₁₀ concentration measurements in Dublin city. *Environ. Monit. Assess.* 52, 3–18. https://doi.org/10.1007/978-94-011-5127-6_1.
- Li, Q., Guan, X., Wu, P., Wang, X., Zhou, L., Tong, Y., et al., 2020. Early transmission dynamics in Wuhan, China, of novel coronavirus-infected pneumonia. *N. Engl. J. Med.* <https://doi.org/10.1056/NEJMoa2001316>.
- Lowen, A.C., Mubareka, S., Steel, J., Palese, P., 2007. Influenza virus transmission is dependent on relative humidity and temperature. *PLoS Pathog.* 3 (10), e151. <https://doi.org/10.1371/journal.ppat.0030151>.
- Luginaah, I.N., Fung, K.Y., Gorey, K.M., Webster, G., Wills, C., 2005. Association of ambient air pollution with respiratory hospitalization in a government-designated "area of concern": the case of Windsor, Ontario. *Environ. Health Perspect.* 113 (3), 290–296. <https://doi.org/10.1289/ehp.7300>.
- Medina-Ramon, M., Zanobetti, A., Schwartz, J., 2006. The effect of ozone and PM₁₀ on hospital admissions for pneumonia and chronic obstructive pulmonary disease: a national multicity study. *Am. J. Epidemiol.* 163 (6), 579–588. <https://doi.org/10.1093/aje/kwj078>.
- Neupane, B., Jerrett, M., Burnett, R.T., Marrie, T., Arain, A., Loeb, M., 2010. Long term exposure to ambient air pollution and risk of hospitalization with community-acquired pneumonia in older adults. *Am. J. Respir. Crit. Care Med.* 181, 47–53. <https://doi.org/10.1164/rccm.200901-0160OC>.
- Notari, A., 2020. Temperature Dependence of COVID-19 Transmission arXiv preprint arXiv:2003.12417. <https://arxiv.org/abs/2003.12417>.
- Pastva, A.M., Wright, J.R., Williams, K.L., 2007. Immunomodulatory roles of surfactant proteins A and D: implications in lung disease. *Proc. Am. Thorac. Soc.* 4 (3), 252–257. <https://doi.org/10.1513/pats.200701-018AW>.
- Pateraki, S., Asimakopoulou, D.N., Flocas, H.A., Maggos, T., Vasilakos, C., 2012. The role of meteorology on different sized aerosol fractions (PM₁₀, PM_{2.5}, PM_{2.5-10}). *Sci. Total Environ.* 419, 124–135. <https://doi.org/10.1016/j.scitotenv.2011.12.064>.
- Piazzalunga-Expert, A., 2020. Evaluation Of the Potential Relationship between Particulate Matter (PM) Pollution and COVID-19 Infection Spread in Italy. Mimeo. http://www.simaonline.it/wpsima/wp-content/uploads/2020/03/COVID_19_position-paper_ENG.pdf.
- Pepe, E., Bajardi, P., Gauvin, L., Privitera, F., Lake, B., Cattuto, C., Tizzoni, M., 2020. COVID-19 Outbreak Response: a First Assessment of Mobility Changes in Italy Following National Lockdown. medRxiv. <https://doi.org/10.1101/2020.03.22.20039933>.
- Pope III, C.A., Dockery, D.W., 2006. Health effects of fine particulate air pollution: lines that connect. *J. Air Waste Manag. Assoc.* 56 (6), 709–742. <https://doi.org/10.1080/10473289.2006.10464485>.
- Pope III, C.A., Ezziati, M., Dockery, D.W., 2009. Fine-particulate air pollution and life expectancy in the United States. *N. Engl. J. Med.* 360 (4), 376–386. <https://doi.org/10.1056/nejmsa0805646>.
- Sayadi, M., Moghbeli, F., Mehrjoo, H., Mahaki, M., 2020. A linear study of the spread of COVID19 in China and Iran. *Front. Health Inform.* 9 (1), 32. <https://doi.org/10.30699/fhi.v9i1.221>.
- Sahin, A.R., Erdogan, A., Agaoglu, P.M., Dineri, Y., Cakirci, A.Y., Senel, M.E., Tasdogan, A.M., 2020. 2019 novel coronavirus (COVID-19) outbreak: a review of the current literature. *EJMO* 4 (1), 1–7. <https://doi.org/10.14744/ejmo.2020.12220>.
- Santus, P., Russo, A., Madonini, E., Allegra, L., Blasi, F., Centanni, S., et al., 2012. How air pollution influences clinical management of respiratory diseases. A case-crossover study in Milan. *Respir. Res.* 13 (1), 95. <https://doi.org/10.1186/1465-9921-13-95>.
- Shaman, J., Kohn, M., 2009. Absolute humidity modulates influenza survival, transmission, and seasonality. *Proc. Natl. Acad. Sci. Unit. States Am.* 106 (9), 3243–3248. <https://doi.org/10.1073/pnas.0806852106>.
- Tsai, D.H., Riediker, M., Berchet, A., Paccaud, F., Waerber, G., Vollenweider, P., Bochud, M., 2019. Effects of short-and long-term exposures to particulate matter on inflammatory marker levels in the general population. *Environ. Sci. Pollut. Control Ser.* 26 (19), 19697–19704. <https://doi.org/10.1007/s11356-019-05194-y>.
- Wang, Q., Taylor, J.E., 2016. Patterns and limitations of urban human mobility resilience under the influence of multiple types of natural disaster. *PLoS One* 11 (1). <https://doi.org/10.1371/journal.pone.0147299>.
- Wu, X., Nethery, R.C., Sabath, B.M., Braun, D., Dominici, F., 2020. Exposure to Air Pollution and COVID-19 Mortality in the United States. medRxiv. <https://doi.org/10.1101/2020.04.05.20054502>.
- Xu, G., Jiao, L., Zhang, B., Zhao, S., Yuan, M., Gu, Y., et al., 2016. Spatial and temporal variability of the PM_{2.5}/PM₁₀ ratio in Wuhan, Central China. *Aerosol Air Qual. Res.* 17 (3), 741–751. <https://doi.org/10.4209/aaqr.2016.09.0406>.
- Zanobetti, A., Schwartz, J., 2006. Air pollution and emergency admissions in Boston, MA. *J. Epidemiol. Community Health* 60 (10), 890–895. <https://doi.org/10.1136/jech.2005.039834>.
- Zehender, G., Lai, A., Bergna, A., Meroni, L., Riva, A., Balotta, C., et al., 2020. Genomic characterization and phylogenetic analysis of SARS-CoV-2 in Italy. *J. Med. Virol.* <https://doi.org/10.1002/jmv.25794>.
- Zeng, X., Xu, X., Zheng, X., Reponen, T., Chen, A., Huo, X., 2016. Heavy metals in PM_{2.5} and in blood, and children's respiratory symptoms and asthma from an e-waste recycling area. *Environ. Pollut.* 210, 346–353. <https://doi.org/10.1016/j.envpol.2016.01.025>.
- Zhang, Y., He, M., Wu, S., Zhu, Y., Wang, S., Shima, M., et al., 2015. Short-term effects of fine particulate matter and temperature on lung function among healthy college students in Wuhan, China. *Int. J. Environ. Res. Publ. Health* 12 (7), 7777–7793. <https://doi.org/10.3390/ijerph120707777>.
- Žuk, T., Rakowski, F., Radomski, J.P., 2009. Probabilistic model of influenza virus transmissibility at various temperature and humidity conditions. *Comput. Biol. Chem.* 33 (4), 339–343. <https://doi.org/10.1016/j.compbiolchem.2009.07.005>.